Ain Shams Engineering Journal 17 (2026) 104019

Contents lists available at ScienceDirect

Ain Shams Engineering Journal

journal homepage: www.sciencedirect.com

Full length article

Theoretical and computational analysis of a novel fractional-order mathematical model for HIV transmission dynamics

Zakirullah [a], Kamal Shah [b,*], M. Motawi Khashan [e], Bahaaeldin Abdalla [b], Thabet Abdeljawad [b,c,d,**]

[a] School of Mathematical Sciences, University of Electronic Science and Technology of China, Chengdu, 611731, China
[b] Department of Mathematics and Sciences, Prince Sultan University, Riyadh 11586, Saudi Arabia
[c] Department of Fundamental Sciences, Faculty of Engineering and Architecture, Istanbul Gelisim University, 34310 Avcilar, Istanbul, Turkey
[d] Department of Medical Research, China Medical University, Taichung 40402, Taiwan
[e] Department of Basic Sciences, Common First Year, King Saud University, Riyadh 11451, Saudi Arabia

ARTICLE INFO

Keywords:
HIV transmission dynamics
CF derivative
Nonlinear least squares method
Banach fixed point theorem
Adams–bashforth method

ABSTRACT

We develop a five-class fractional mathematical model to investigate HIV transmission using the Caputo–Fabrizio (CF) derivative. The population is divided into susceptible, acute, chronic, treated and AIDS classes to capture the key stages of HIV progression and the effects of antiretroviral therapy. Existence and uniqueness of solutions are established using the fixed point theorem, a bounded invariant region is identified, and the basic reproduction threshold R_0 is derived using the next-generation matrix. Analytical results demonstrate the local and global stability of both the infection-free equilibrium and the endemic equilibrium. Lower fractional orders are shown to slow convergence to equilibrium, reflecting the memory effects inherent in fractional dynamics. The CF operator therefore provides a flexible and realistic framework for understanding HIV transmission and assessing the influence of treatment, disease progression, and memory effects on long-term epidemic outcomes. The Ulam–Hyers (UH) stability of the considered HIV model under CF derivative is proved. In addition, numerical solutions are obtained by using the Adams–Bashforth method corresponding to the CF derivative. Simulations show that early initiation of antiretroviral therapy, reduced treatment dropout, and improved viral suppression substantially decrease HIV prevalence.

1. Introduction

Over the past decades, HIV/AIDS has continued to pose one of the most persistent global health challenges, with millions of individuals affected worldwide despite remarkable advances in prevention and treatment. The epidemiology of HIV is shaped by a complex interplay between biological, behavioral, and therapeutic factors, which makes its control particularly difficult [1]. HIV attacks and destroys CD4 T cells in the human immune system, leading to severe immune suppression and greater vulnerability to infections and diseases. Mortality remains high, and no effective cure for HIV/AIDS has been developed to date. Since its first recognition by the Centers for Disease Control and Prevention in 1981, AIDS has become a global pandemic [2]. The World Health Organization reported that by the end of 2022, approximately 39 million people were living with HIV worldwide, with around 1.3 million new infections and 630,000 AIDS-related deaths in that year. In 2023, an estimated 37.7 million people were living with HIV/AIDS worldwide, with roughly 1.5 million new infections each year. Sub-Saharan Africa continues to bear the greatest impact, accounting for about 67% of global cases (we refer to [3]). Data from the Chinese Center for Disease Control and Prevention indicate that China recorded 1.223 million people living with HIV and 418,000 cumulative deaths by the end of 2022. These figures continue to grow, highlighting the pressing public health threat of AIDS in China [4].

HIV is transmitted mainly through mother-to-child contact, blood exposure, and sexual activity. According to a 2018 report from China's National Health Commission, blood and mother-to-child transmission are now well controlled, making sexual transmission, both heterosexual and homosexual, the dominant route [5]. Data from the Data Center for

* Corresponding author.
** Corresponding author at: Department of Mathematics and Sciences, Prince Sultan University, Riyadh 11586, Saudi Arabia.
Email addresses: zakirullahbzt@gmail.com (Zakirullah), kshah@psu.edu.sa (K. Shah), khashan@ksu.edu.sa (M. Motawi Khashan), babdallah@psu.edu.sa (B. Abdalla), tabdeljawad@psu.edu.sa (T. Abdeljawad).

https://doi.org/10.1016/j.asej.2026.104019
Received 29 September 2025; Received in revised form 31 December 2025; Accepted 27 January 2026
Available online 11 February 2026

Public Health Sciences show that in 2022, sexual transmission accounted for 97.6% of new infections, with heterosexual contact responsible for 72.0% and homosexual contact for 25.6% (see [6]). A notable shift is the rising proportion of HIV/AIDS cases among older adults. In 2005, people aged 60 and above made up only 6.3% of cases, but by 2020 this share had climbed to 44% [7]. Investigating the role of the elderly in HIV/AIDS transmission is therefore increasingly important. To strengthen prevention and control, researchers have concentrated on three key areas [8]. Experimental studies explore cellular structures that affect disease progression. Descriptive studies analyze data to identify underlying drivers [9].

Mathematical modeling has become an indispensable tool for dissecting the dynamics of HIV infection and evaluating control strategies [10]. In modern society, mathematical modeling plays an important role in analyzing disease dynamics, transmission patterns, testing interventions and evaluating treatment effects [11,12]. The long-term consequences of public health policies are forecasted using models that incorporate transmission rates, medication adherence and behavioral modifications. Rihan [13] studied numerical analysis of biological modeling. Eaton et al. [14] studied antiviral therapy for HIV incidence in South Africa. Hyman and Stanley [15] constructed a mathematical model of AIDS. The traditional epidemic model, however, often fails to capture real-world dynamics, as it fails to take into account critical factors such as the effect of previous disease spread on new infections and regional variations in transmission. For instance, Odebiyi et al. [16] studied screening of HIV/AIDS by using mathematical models. Zanib et al. [17] conducted comprehensive analysis of HIV/AIDS. Also, Meetei et al. [18] studied and analyzed simulations of HIV/AIDS by using real cases. Recent studies have applied fractional order derivatives for investigating HIV and other infectious diseases by using mathematical model. The mentioned tools have highlighted the role of memory and nonlocal effects in disease persistence. Yang et al. [19] studied Chlamydia psittaci and KPC producing gram negative bacteria infection using mathematical model. Xu et al. [20] investigated SARS-CoV-2 omicron variant infection during pregnancy in women. Ullah et al. [21] studied a new co-infection model for HBV and HIV with vaccination. Shi et al. [22] investigated hypergraph-based model for modeling multi-agent q-learning dynamics in public goods games. Authors [23] established a new sepsis screening tool based on lymphocyte count mathematical model. Researchers [24] studied a bacteria infection through mathematical model. Shukla and Sukavanam [25] studied controllability results for a system. Authors [26] deduced the existence and controllability results for a problem under Atangana-Baleanu derivative. Chauhan [27] analyzed memory based dynamical system of coffee berry disease. Researchers [28] studied fractional order HIV/AIDS model. Almuallem et al. [29] used fractional order model to study effects of quarantine and vaccination on the transmission of Lumpy skin disease. Chauhan et al. [30] used CF fractional order derivative to study financial mathematical model. Kumar et al. [31] studied TB model under fractional derivative. Boulaaras et al. [32] investigated stability results for an autonomous system. Authors [33] studied liver transplantation in HIV-AIDS through mathematical model. Selvam et al. [34] studied stability analysis of financial mathematical model. In addition, an Ebola mathematical model under fractional derivative was studied by Selvam and his coauthors [35]. UH stability was investigated for tuberculosis disease model using fractional derivative [36].

In such scenarios, fractional-order models demonstrate considerable benefits. Authors [37] studied nonlinear wave dynamics by using fractional derivative. Deterministic fractional compartmental models illustrate these long-term dependencies and allow for more accurate and comprehensive analysis than classical models. For instance Boulaaras et al. [38] studied UH stability for Chen system. Fractional mathematical modeling has emerged as a crucial tool in epidemiology to address these complexities [39,40]. It also provides a valuable framework for evaluating the dynamics of infection, transmission patterns, and the potential impact of interventions. Numerous scientific disciplines have gained interest in FDEs [41]. By employing fractional-order derivatives, complex systems can be demonstrated as more accurate systems in comparison to using traditional integer-order derivatives, providing significant insights for healthcare providers and policymakers attempting to limit morbidity and mortality from HIV (we refer to [42]). Provide a systematic approach to represent population-level dynamics by partitioning individuals into epidemiologically relevant classes and describing their transitions among the compartments. In this regard, for some useful results, we refer readers to [43,44].

Our research presents a five class HIV model under the CF fractional derivative, which captures the nonlocal temporal influence of past infection history without the singular kernel characteristic of classical fractional operators, and introduces distinct relative infectiousness parameters that reflect differences in viral load and behavioral patterns across these stages. This formulation enables a more accurate representation of how treatment and disease progression jointly affect transmission potential. Mathematically, we provide a rigorous analysis of the existence and uniqueness of solutions via the fixed'point theorem, identify a positively invariant bounded region to ensure biological feasibility, and derive the R_0 using the next-generation matrix approach. The equilibria points of local stability are established via the Jacobian approach, and global stability through the Lyapunov function approach is established and the UH stability of the fractional system is proven, guaranteeing that the CF system is well-posed and that small perturbations or numerical errors do not lead to large deviations in the solution. Numerical simulations using the Adams-Bashforth scheme for the CF derivative further reveal the influence of memory order and treatment control on epidemic dynamics.

The rest of the manuscript is organized as follows. In Section 1.1, we review the fundamental concepts of fractional derivatives used in this work. The proposed HIV model, including variable definitions and the full model formulation, estimation, and data fitting, appears in Section 2. Mathematical properties, positivity, and boundedness are established in Section 2.2. In Section 2.3, we derive equilibria and the basic reproduction threshold. Section 3 addresses the existence and uniqueness of solutions as well as their UH stability. Section 4 provides a detailed stability analysis. The numerical scheme is described in Section 5, followed by numerical simulations and discussion in Section 6. We conclude with a summary of the main findings in Section 7.

1.1. Definitions and preliminary concepts

We employ the CF fractional derivative [45,46]. For a function $h \in H^1(a,b)$, the CF derivative of order $\varsigma \in (0,1)$ is defined as

$$ {}^{CF}D_t^{\varsigma} f(t) = \frac{U(\varsigma)}{1-\varsigma} \int_a^t f'(x) \exp\left(-\frac{\varsigma(t-x)}{1-\varsigma}\right) dx, \tag{1}$$

where $U(\varsigma)$ is a normalization function satisfying $U(0) = U(1) = 1$. An equivalent form can be obtained by setting $\alpha = \frac{1-\varsigma}{\varsigma}$, which yields

$$ {}^{CF}D_t^{\varsigma} f(t) = \frac{M(\alpha)}{\alpha} \int_a^t f'(x) \exp\left(-\frac{t-x}{\alpha}\right) dx, \quad M(0) = M(\infty) = 1, \tag{2}$$

demonstrating the exponential, non-singular kernel structure. In the limit $\alpha \to 0$, the kernel reduces to a Dirac distribution:

$$\lim_{\alpha \to 0} \frac{1}{\alpha} \exp\left(-\frac{t-x}{\alpha}\right) = \delta(t-x).$$

The associated CF fractional integral of order $\varsigma \in (0,1)$ for a function g is given by

$$ {}^{CF}I_t^{\varsigma} g(t) = \frac{2(1-\varsigma)}{(2-\varsigma)U(\varsigma)} g(t) + \frac{2\varsigma}{(2-\varsigma)U(\varsigma)} \int_0^t g(u)\, du, \tag{3}$$

with the normalization condition

$$\frac{2(1-\varsigma)}{(2-\varsigma)U(\varsigma)} + \frac{2\varsigma}{(2-\varsigma)U(\varsigma)} = 1. \tag{4}$$

2. Model formulation

To describe the transmission dynamics of HIV, we developed a compartmental model that stratifies the human population into five mutually exclusive epidemiological classes. At any time t, the total population $N(t)$ is expressed as

$$N(t) = S(t) + I(t) + C(t) + T(t) + A(t),$$

where $S(t)$ denotes susceptible individuals, $I(t)$ represents individuals in the acute infection stage, $C(t)$ corresponds to those in the long-term chronic stage, $T(t)$ denotes individuals receiving antiretroviral therapy (ART), and $A(t)$ represents individuals with advanced HIV infection or AIDS. The model assumptions and transitions between compartments are illustrated in Fig. 1.

Transmission of HIV occurs through effective contact between susceptible individuals and those who are infectious. The force of infection, which quantifies the per capita rate at which susceptible individuals acquire infection, is given by

$$\psi(t) = \frac{\beta}{N(t)} \left(\varepsilon_I I + \varepsilon_C C + \varepsilon_T T + \varepsilon_A A\right), \tag{5}$$

where β is the effective contact rate, and ε_j ($j \in \{I, C, T, A\}$) are weighting parameters that represent the relative infectiousness of individuals in the acute, chronic, treatment, and AIDS stages, respectively. The inclusion of the relative infectiousness coefficients $\varepsilon_I, \varepsilon_C, \varepsilon_T$, and ε_A accounts for known biological heterogeneity in HIV transmission potential across stages of infection. Individuals in the acute infection stage (I) exhibit extremely high viral loads and are thus the most infectious; those in the chronic stage (C) maintain a lower but sustained infectiousness. Persons undergoing ART (T) have strong viral suppression, leading to significantly reduced transmissibility ($\varepsilon_T \ll 1$), while individuals with AIDS (A) may remain infectious but often experience reduced contact activity. Hence, the expected qualitative relationship is

$$\varepsilon_I > \varepsilon_C > \varepsilon_A > \varepsilon_T.$$

This stratification allows the model to capture stage-specific transmission dynamics and to assess the contribution of treatment and disease progression to the overall epidemic. The susceptible population increases through recruitment at rate Λ and decreases due to infection and natural death at rate μ:

$$\frac{dS}{dt} = \Lambda - \psi S - \mu S. \tag{6}$$

Here, ψ is the force of infection defined in (5).

Susceptible individuals become acutely infected following exposure. Acutely infected individuals may progress to the chronic stage at rate γ_{IC}, initiate ART at rate τ_I, or die due to natural and disease-induced causes at rates μ and α_I, respectively:

$$\frac{dI}{dt} = \psi S - (\mu + \gamma_{IC} + \tau_I + \alpha_I) I. \tag{7}$$

Individuals enter the chronic stage from the acute stage at rate γ_{IC}. They may progress to AIDS at rate γ_{CA}, initiate ART at rate τ_C, revert from treatment at rate ρ, or die naturally or from disease at rates μ and α_C, respectively:

$$\frac{dC}{dt} = \gamma_{IC} I - (\mu + \gamma_{CA} + \tau_C + \alpha_C) C + \rho T. \tag{8}$$

Treatment may be initiated during any infection stage at respective rates τ_I, τ_C, and τ_A. Treated individuals may discontinue therapy or experience treatment failure at rate ρ, progress to AIDS at rate θ_T, or die at rate μ:

$$\frac{dT}{dt} = \tau_I I + \tau_C C + \tau_A A - (\mu + \rho + \theta_T) T. \tag{9}$$

AIDS cases arise from chronic progression and treatment failure. Individuals with AIDS may initiate ART at rate τ_A, die from AIDS-related causes at rate δ, or experience natural mortality at rate μ:

$$\frac{dA}{dt} = \gamma_{CA} C + \theta_T T - (\mu + \delta + \tau_A + \alpha_A) A. \tag{10}$$

The set of Eqs. (6)–(10) together with (5) constitutes the proposed fractional order model describing the transmission dynamics of HIV (Fig. 2).

$$\begin{aligned}
&{}^{CF}D_t^{\varsigma} S = \Lambda - \psi S - \mu S,\\
&{}^{CF}D_t^{\varsigma} I = \psi S - (\mu + \gamma_{IC} + \tau_I + \alpha_I) I,\\
&{}^{CF}D_t^{\varsigma} C = \gamma_{IC} I - (\mu + \gamma_{CA} + \tau_C + \alpha_C) C + \rho T,\\
&{}^{CF}D_t^{\varsigma} T = \tau_I I + \tau_C C + \tau_A A - (\mu + \rho + \theta_T) T,\\
&{}^{CF}D_t^{\varsigma} A = \gamma_{CA} C + \theta_T T - (\mu + \delta + \tau_A + \alpha_A) A,
\end{aligned} \tag{11}$$

The system is considered with nonnegative initial conditions:

$$S(0) = S_0, \quad I(0) = I_0, \quad C(0) = C_0, \quad T(0) = T_0, \quad A(0) = A_0.$$

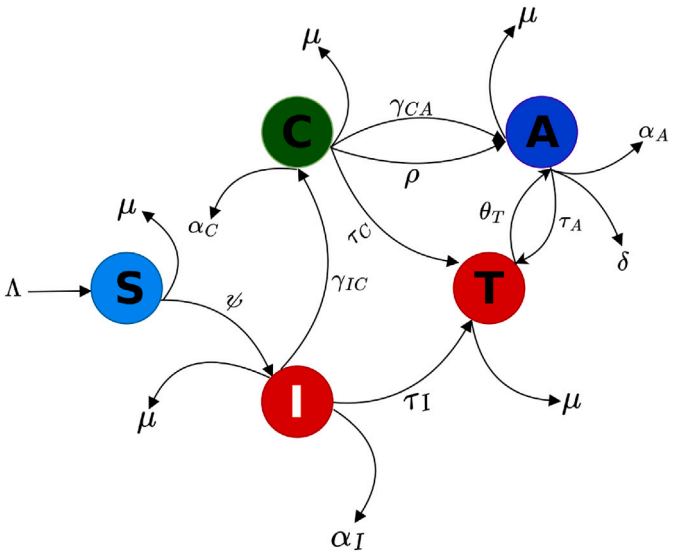

Fig. 1. Schematic diagram of HIV transmission and progression between epidemiological classes.

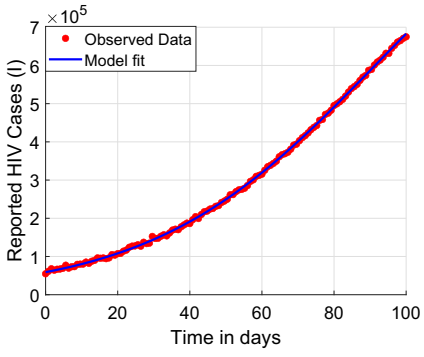

Fig. 2. Model fit to observed infection of HIV and solid line represents model-predicted infections, and the dots represent observed reported cases when $\varsigma = 1$.

2.1. Parameter estimation using nonlinear least squares (NLS)

Estimation of the epidemiological parameters governing the model (11), we employed an NLS approach using the observed data provided by Cai et al. [47]. Furthermore, we solve the following optimization problem (Fig. 2):

$$\mathfrak{J}(\Bbbk) = \sum_{j=1}^{T} \left\| y(t_j) - \hbar(\Bbbk, x(t_j)) \right\|^2 \tag{12}$$

⇒ Simulate the model using an initial guess of the parameters $\Bbbk$ to generate the state variables $x(t_j)$, and compute the observable outputs $\hbar(\Bbbk, x(t_j))$.
⇒ Compute the discrepancy between the observed data $y(t_j)$ and the model predictions $\hbar(\Bbbk, x(t_j))$, then form the objective (cost) function $\mathfrak{J}(\Bbbk)$.
⇒ Minimize the cost function $\mathfrak{J}(\Bbbk)$ using nonlinear optimization techniques to obtain the best-fit parameters $\hat{\Bbbk}$, which are then used to perform curve fitting and validate the model. We fit the parameters shown in Table 1.

2.2. Positivity and feasible region

In this section, we discuss positivity and feasible region.

Theorem 2.1. *Let the initial data satisfy*

$$S(0) > 0, \qquad I(0) \geq 0, \qquad C(0) \geq 0, \qquad T(0) \geq 0, \qquad A(0) \geq 0,$$

and denote the positive orthant

$$\Omega = \left\{ (S, I, C, T, A) \in \mathbb{R}^5_+ \right\}.$$

Then the solution of system (11) satisfies the following properties for all $t \geq 0$:

(i) Positivity: the solution remains in Ω.

(ii) Uniform boundedness: there exists a finite constant

$$K = \frac{\Lambda}{\mu} > 0,$$

depending only on the recruitment rate A and the natural removal rate μ, such that the total population $N(t) = S(t)+I(t)+C(t)+T(t)+A(t)$ satisfies $N(t) \leq K$ for all $t \geq 0$. Consequently, each compartment is uniformly bounded by K.

Hence the region $\Omega_K := \{(S, I, C, T, A) \in \Omega : \ S + I + C + T + A \leq K\}$ is positively invariant for system (11).

Proof. let N(t) denote the total population. Summing the model in (11) yields a fractional differential inequality of the form

$${}^{CF}_{0}D^{\varsigma}_{t}\mathcal{N}(t) \leq \Lambda - \mu\mathcal{N}(t),$$

implying that $\mathcal{N}(t)$ is ultimately bounded above by Λ/μ. More precisely,

$$\mathcal{N}(t) \leq \left(\mathcal{N}(0) - \frac{\Lambda}{\mu} \right) E_{\varsigma}(-\mu t) + \frac{\Lambda}{\mu},$$

where E_{ς} denotes the Mittag-Leffler function. This guarantees that the total population approaches the feasible region asymptotically and remains within it thereafter.

We therefore define the biologically feasible region as

$$\Omega = \left\{ (S, I, C, T, A) \in \mathbb{R}^5_+ : 0 \leq \mathcal{N}(t) \leq \frac{\Lambda}{\mu} \right\}.$$

Within Ω, the model dynamics are well posed and biologically meaningful. Furthermore, since Ω is positively invariant, any trajectory of the system that starts and remains in Ω. Consequently, each compartment is also bounded by K, and the set Ω_K is positively invariant.

$${}^{CF}_{0}D^{\varsigma}_{t}S\Big|_{S=0} = \Lambda \geq 0,$$
$${}^{CF}_{0}D^{\varsigma}_{t}I\Big|_{S=0} = \psi S \geq 0,$$
$${}^{CF}_{0}D^{\varsigma}_{t}C\Big|_{S=0} = \gamma_{IC} I + \rho T \geq 0,$$
$${}^{CF}_{0}D^{\varsigma}_{t}T\Big|_{S=0} = \tau_I I + \tau_C C + \tau_A A \geq 0,$$
$${}^{CF}_{0}D^{\varsigma}_{t}A\Big|_{S=0} = \gamma_{CA} C + \theta_T T \geq 0.$$

□

Table 1
Description of model parameters in the five-class HIV transmission framework.

Parameter	Biological meaning	Value (per day)	Source
Λ	Recruitment rate	$537915 \times \frac{1}{365}$	[48]
μ	Natural mortality rate	$\frac{1}{79 \times 365}$	[49]
β	Baseline transmission rate	0.005	Fitted
ϵ_I	Relative infectiousness of acute stage	0.038	Fitted
ϵ_C	Relative infectiousness of chronic stage	0.3	Fitted
ϵ_T	Relative infectiousness under ART	0.04	Fitted
ϵ_A	Relative infectiousness of AIDS stage	0.500	Fitted
γ_{IC}	Progression rate from acute to chronic stage	0.100	Fitted
γ_{CA}	Progression rate from chronic to AIDS stage	0.030	Fitted
τ_I	ART initiation rate for acute stage	0.052	Fitted
τ_C	ART initiation rate for chronic stage	0.020	Fitted
τ_A	ART initiation rate for AIDS stage	0.030	Fitted
ρ	ART discontinuation or treatment failure rate	0.003	Fitted
θ_T	Progression rate from ART to AIDS	0.020	Fitted
α_I	Disease-induced mortality in acute stage	0.010	Fitted
α_C	Disease-induced mortality in chronic stage	0.031	Fitted
α_A	Disease-induced mortality in AIDS stage	0.045	Fitted
δ	Additional AIDS-related mortality rate	0.0005945	[50]

2.3. Equilibria and threshold reproduction

In this section, we discuss equilibria and threshold reproduction (R_0). The infection-free equilibrium point is the steady state at which no infection is present in the population, all infected compartments are zero while persistent-infection is the steady state at which the disease persists at constant positive levels in one or more infected compartments. Threshold reproduction is the expected number of secondary infections produced by a single infectious individual in a fully susceptible population.

Theorem 2.2. *The system (11) admits a unique infection-free equilibrium point for $R_0 < 1$ and a unique persistent-infection equilibrium point for $R_0 > 1$.*

Proof. To compute the infection-free equilibrium point, we set all infected compartments equal to zero:

$${}^{CF}D^{\varsigma}_{0}S = {}^{CF}D^{\varsigma}_{0}I = {}^{CF}D^{\varsigma}_{0}C = {}^{CF}D^{\varsigma}_{0}T = {}^{CF}D^{\varsigma}_{0}A = 0 \tag{13}$$

Solving (13) gives the infection-free equilibrium point, denoted E_0, for which the following expressions hold:

$$E_0 = \left(\frac{\Lambda}{\mu}, 0, 0, 0, 0 \right) \tag{14}$$

We now proceed to derive the persistent-infection equilibrium point, where all compartments are nonzero:

$$ {}^{CF}D_0^{\varsigma} S \neq {}^{CF}D_0^{\varsigma} I \neq {}^{CF}D_0^{\varsigma} C \neq {}^{CF}D_0^{\varsigma} T \neq {}^{CF}D_0^{\varsigma} A \neq 0 \tag{15}$$

The persistent-infection equilibrium point is calculated using back substitution, yielding E^*, with the components given by:

$$S^* = \frac{\Lambda}{(\psi^* + \mu)}$$

$$C^* = \frac{\rho\Theta_4\tau_I I^* - \Theta_3\Theta_4 I^*\gamma_{CI} + \tau_A\theta_T I^*\gamma_{CI}}{\rho\tau_A\tau_C - \rho\Theta_4\tau_C - \Theta_2\Theta_3\Theta_4 + \Theta_2\tau_A\theta_T}$$

$$T^* = \frac{\tau_A\tau_C I^*\gamma_{CI} - \Theta_4\tau_C I^*\gamma_{CI} - \Theta_2\Theta_4\tau_I I^*}{\rho\tau_A\tau_C - \rho\Theta_4\tau_C - \Theta_2\Theta_3\Theta_4 + \Theta_2\tau_A\theta_T}$$

$$A^* = \frac{\tau_A\tau_C I^*\gamma_{CI} - \Theta_4\tau_C I^*\gamma_{CI} - \Theta_2\Theta_4\tau_I I^*}{\rho\tau_A\tau_C - \rho\Theta_4\tau_C - \Theta_2\Theta_3\Theta_4 + \Theta_2\tau_A\theta_T}.$$

By substituting C^*, T^*, and A^* into Eq. (5), we obtain

$$I^* = \frac{\psi N(\rho\tau_A\tau_C - \rho\Theta_4\tau_C - \Theta_2\Theta_3\Theta_4 + \Theta_2\tau_A\theta_T)}{\begin{array}{l}\beta(\varepsilon_I + \varepsilon_C(\rho\Theta_4\tau_I - \Theta_3\Theta_4\gamma_{CI} + \tau_A\theta_T\gamma_{CI}) \\ +\varepsilon_T(\tau_A\tau_C - \Theta_4\tau_{CCI} - \Theta_2\Theta_4\tau_I) + \varepsilon_A(\tau_A\tau_{CCI} - \Theta_4\tau_{CCI} - \Theta_2\Theta_4\tau_I))\end{array}}.$$

Here, S^*, I^*, C^*, T^*, A^*, ensure the existence of a biologically feasible persistent-infection equilibrium point. □

2.4. Threshold reproduction (R_0)

To compute the threshold reproduction, denoted by R_0, using the *next-generation matrix method* [51]. This approach expresses R_0 as the spectral radius of the matrix product FV^{-1}, that is,

$$R_0 = \rho(FV^{-1}),$$

where ρ denotes the spectral radius, and the matrices F and V are defined as

$$F = \begin{pmatrix} \beta\varepsilon_I & \beta\varepsilon_C & \beta\varepsilon_T & \beta\varepsilon_A \\ 0 & 0 & 0 & 0 \\ 0 & 0 & 0 & 0 \\ 0 & 0 & 0 & 0 \end{pmatrix},$$

$$V = \begin{pmatrix} \mu + \gamma_{IC} + \tau_I + \alpha_I & 0 & 0 & 0 \\ -\gamma_{IC} & \mu + \gamma_{CA} + \tau_C + \alpha_C & -\rho & 0 \\ -\tau_I & -\tau_C & \mu + \rho + \theta_T & -\tau_A \\ 0 & -\gamma_{CA} & -\theta_T & \mu + \delta + \tau_A + \alpha_A \end{pmatrix}.$$

The inverse of V is given by

$$V^{-1} = \begin{pmatrix} \frac{1}{\mu+\gamma_{IC}+\tau_I+\alpha_I} & 0 & 0 & 0 \\ \frac{\Delta_1}{\Delta_2} & \frac{(\mu+\rho+\theta_T)(\mu+\delta+\tau_A+\alpha_A)-\tau_A\theta_T}{\Delta_5} & \frac{\rho(\mu+\delta+\tau_A+\alpha_A)}{\Delta_5} & \frac{\rho\tau_A}{\Delta_5} \\ \frac{\Delta_3}{\Delta_2} & \frac{\tau_A\gamma_{AC}+(\mu+\delta+\tau_A+\alpha_A)\tau_C}{\Delta_5} & \frac{(\mu+\gamma_{CA}+\tau_C+\alpha_C)(\mu+\delta+\tau_A+\alpha_A)}{\Delta_5} & \frac{(\mu+\gamma_{CA}+\tau_C+\alpha_C)\tau_A}{\Delta_5} \\ \frac{\Delta_4(\rho\gamma_{AC}+\theta_T\mu+\theta_T\gamma_{CA}+\theta_T\tau_C+\theta_T\alpha_C)}{\Delta_5(\mu+\gamma_{IC}+\tau_I+\alpha_I)(\rho\gamma_{AC}+\mu\theta_T+\theta_T\gamma_{CA}+\theta_T\tau_C+\alpha_C\theta_T)} & \frac{(\mu+\rho+\theta_T)\gamma_{AC}+\tau_C\theta_T}{\Delta_5} & \frac{\rho\gamma_{AC}+(\mu+\gamma_{CA}+\tau_C+\alpha_C)\theta_T}{\Delta_5} & \frac{(\mu+\gamma_{CA}+\tau_C+\alpha_C)(\mu+\rho+\theta_T)-\rho\tau_C}{\Delta_5} \end{pmatrix},$$

where,

$$\begin{aligned}
\Delta_1 &= \tau_A\theta_T\gamma_{CI} - \rho(\mu+\delta+\tau_A+\alpha_A)\tau_I - (\mu+\rho+\theta_T)(\mu+\delta+\tau_A+\alpha_A)\gamma_{CI}, \\
\Delta_2 &= (\mu+\gamma_{IC}+\tau_I+\alpha_I)((\mu+\gamma_{CA}+\tau_C+\alpha_C)(\mu+\rho+\theta_T)(\mu+\delta+\tau_A+\alpha_A) \\
&\quad - \rho\tau_A\gamma_{AC} - \rho(\mu+\delta+\tau_A+\alpha_A)\tau_C - (\mu+\gamma_{CA}+\tau_C+\alpha_C)\tau_A\theta_T), \\
\Delta_3 &= \tau_A\gamma_{AC}\gamma_{CI} + ((\mu+\gamma_{CA}+\tau_C+\alpha_C)\tau_I + 1)(\mu+\delta+\tau_A+\alpha_A)\tau_C\gamma_{CI}, \\
\Delta_4 &= \rho\tau_I\gamma_{AC} + (\mu+\rho+\theta_T)\gamma_{AC}\gamma_{CI} + (\mu+\gamma_{CA}+\tau_C+\alpha_C)\theta_T\tau_I + \tau_C\theta_T\gamma_{CI}, \\
\Delta_5 &= (\mu+\gamma_{CA}+\tau_C+\alpha_C)(\mu+\rho+\theta_T)(\mu+\delta+\tau_A+\alpha_A) - \rho\tau_A\gamma_{AC} \\
&\quad - \rho(\mu+\delta+\tau_A+\alpha_A)\tau_C - (\mu+\gamma_{CA}+\tau_C+\alpha_C)\tau_A\theta_T.
\end{aligned}$$

After computing the product FV^{-1}, the dominant eigenvalue (spectral radius) is obtained as

$$R_0 = \frac{\beta(\Delta_1\Delta_5\varepsilon_C + \Delta_3\Delta_5\varepsilon_T)(\mu+\gamma_{IC}+\tau_I+\alpha_I) + \Delta_2\Delta_4\beta\varepsilon_A + \Delta_2\Delta_5\beta\varepsilon_I}{\Delta_2\Delta_5(\mu+\gamma_{IC}+\tau_I+\alpha_I)}$$

After substituting the parameter values from Table 1, the threshold reproduction is $R_0 = 0.0017$, indicating that the infection cannot sustain itself in the population.

3. Existence and uniqueness of solutions

By applying the fixed-point method to the equivalent integral system, we rigorously demonstrate that the model (11) admits a unique solution under appropriate conditions.

$$\begin{aligned}
S(t) &= S_0 + {}^{CF}J_t^{\varsigma}(\Lambda - \psi S - \mu S), \\
I(t) &= I_0 + {}^{CF}J_t^{\varsigma}(\psi S - (\mu+\gamma_{IC}+\tau_I+\alpha_I)I), \\
C(t) &= C_0 + {}^{CF}J_t^{\varsigma}(\gamma_{IC}I - (\mu+\gamma_{CA}+\tau_C+\alpha_C)C + \rho T), \\
T(t) &= T_0 + {}^{CF}J_t^{\varsigma}(\tau_I I + \tau_C C + \tau_A A - (\mu+\rho+\theta_T)T), \\
A(t) &= A_0 + {}^{CF}J_t^{\varsigma}(\gamma_{CA}C + \theta_T T - (\mu+\delta+\tau_A+\alpha_A)A).
\end{aligned} \tag{16}$$

Applying Eq. (3) to Eqs. (16) yields

$$\begin{aligned}
S(t) &= S(0) + \frac{2(1-\varsigma)}{(2-\varsigma)\mathcal{M}(\varsigma)}(\Lambda - \psi S - \mu S) \\
&\quad + \frac{2\varsigma}{(2-\varsigma)\mathcal{M}(\varsigma)}\int_0^t (\Lambda - \psi S - \mu S)dy, \\
I(t) &= I(0) + \frac{2(1-\varsigma)}{(2-\varsigma)\mathcal{M}(\varsigma)}(\psi S - (\mu+\gamma_{IC}+\tau_I+\alpha_I)I) \\
&\quad + \frac{2\varsigma}{(2-\varsigma)\mathcal{M}(\varsigma)}\int_0^t (\psi S - (\mu+\gamma_{IC}+\tau_I+\alpha_I)I)dy, \\
C(t) &= C(0) + \frac{2(1-\varsigma)}{(2-\varsigma)\mathcal{M}(\varsigma)}(\gamma_{IC}I - (\mu+\gamma_{CA}+\tau_C+\alpha_C)C + \rho T) \\
&\quad + \frac{2\varsigma}{(2-\varsigma)\mathcal{M}(\varsigma)}\int_0^t (\gamma_{IC}I - (\mu+\gamma_{CA}+\tau_C+\alpha_C)C + \rho T)dy, \\
T(t) &= T(0) + \frac{2(1-\varsigma)}{(2-\varsigma)\mathcal{M}(\varsigma)}(\tau_I I + \tau_C C + \tau_A A - (\mu+\rho+\theta_T)T) \\
&\quad + \frac{2\varsigma}{(2-\varsigma)\mathcal{M}(\varsigma)}\int_0^t (\tau_I I + \tau_C C + \tau_A A - (\mu+\rho+\theta_T)T)dy, \\
A(t) &= A(0) + \frac{2(1-\varsigma)}{(2-\varsigma)\mathcal{M}(\varsigma)}(\gamma_{CA}C + \theta_T T - (\mu+\delta+\tau_A+\alpha_A)A)
\end{aligned} \tag{17}$$

$$+\frac{2\varsigma}{(2-\varsigma)\mathcal{M}(\varsigma)}\int_0^t(\gamma_{CA}C+\theta_T T-(\mu+\delta+\tau_A+\alpha_A)A)dy,$$

We define the kernels as

$$\begin{aligned}
\Upsilon_1(t,S)&=(\Lambda-\psi S-\mu S),\\
\Upsilon_2(t,I)&=\psi S-(\mu+\gamma_{IC}+\tau_I+\alpha_I)I,\\
\Upsilon_3(t,C)&=\gamma_{IC}I-(\mu+\gamma_{CA}+\tau_C+\alpha_C)C+\rho T,\\
\Upsilon_4(t,T)&=\tau_I I+\tau_C C+\tau_A A-(\mu+\rho+\theta_T)T,\\
\Upsilon_5(t,A)&=\gamma_{CA}C+\theta_T T-(\mu+\delta+\tau_A+\alpha_A)A.
\end{aligned}\tag{18}$$

Theorem 3.1. *Let the kernels*

$$\Upsilon_1,\ \Upsilon_2,\ \Upsilon_3,\ \Upsilon_4,\ \Upsilon_5$$

each satisfy the Lipschitz condition. Then, every kernel is a contraction if

$$0\le\Lambda+M+\mu<1.$$

Proof. To establish the desired result, take S and S_1 and consider the operator Υ_1 in the form

$$\Upsilon_1(t,S)-\Upsilon_1(t,S_1)=-\Lambda\left(S(t)-S_1(t)\right)-\psi\left(S(t)-S_1(t)\right)-\mu\left(S(t)-S_1(t)\right).\tag{19}$$

Simplifying (19) yields

$$\begin{aligned}
\left\|\Upsilon_1(t,S)-\Upsilon_1(t,S_1)\right\|&\le\left\|\Lambda\left(S(t)-S_1(t)\right)\right\|\\
&\quad-\left\|\psi\left(S(t)-S_1(t)\right)\right\|-\left\|\mu\left(S(t)-S_1(t)\right)\right\|,\\
&\le\|\Lambda\|\left\|\left(S(t)-S_1(t)\right)\right\|-\|\psi\|\left\|\left(S(t)-S_1(t)\right)\right\|\\
&\quad-\|\mu\|\left\|\left(S(t)-S_1(t)\right)\right\|,\\
&\le\|\Lambda\|\left\|\left(S(t)-S_1(t)\right)\right\|-\|M\|\left\|\left(S(t)-S_1(t)\right)\right\|\\
&\quad-\|\mu\|\left\|\left(S(t)-S_1(t)\right)\right\|,\\
&\le(\Lambda+M+\mu)\left\|\left(S(t)-S_1(t)\right)\right\|,
\end{aligned}\tag{20}$$

Set $\mu_1=\Lambda+M+\mu$. Then

$$\left\|\Upsilon_1(t,S)-\Upsilon_1(t,S_1)\right\|\le\mu_1\left\|S(t)-S_1(t)\right\|.\tag{21}$$

Thus Υ_1 satisfies the Lipschitz condition, and if

$$0\le M+\mu+\psi<1,$$

the mapping is a contraction as required in the CF derivative.

By the same reasoning, the remaining operators satisfy

$$\begin{aligned}
\left\|\Upsilon_2(t,I)-\Upsilon_2(t,I_1)\right\|&\le\mu_2\left\|I(t)-I_1(t)\right\|,\\
\left\|\Upsilon_3(t,C)-\Upsilon_3(t,C_1)\right\|&\le\mu_3\left\|C(t)-C_1(t)\right\|,\\
\left\|\Upsilon_4(t,T)-\Upsilon_4(t,T_1)\right\|&\le\mu_4\left\|T(t)-T_1(t)\right\|,\\
\left\|\Upsilon_5(t,A)-\Upsilon_5(t,A_1)\right\|&\le\mu_5\left\|A(t)-A_1(t)\right\|.
\end{aligned}\tag{22}$$

Each constant μ_i, $i=2,\dots,5$, satisfies $\mu_i<1$. Using these bounds and applying the CF integral operator to Eq. (17) gives

$$\begin{aligned}
S(t)&=S(0)+\frac{2(1-\varsigma)}{(2-\varsigma)\mathcal{Z}(\varsigma)}\Upsilon_1(t,S)+\frac{2\varsigma}{(2-\varsigma)\mathcal{Z}(\varsigma)}\int_0^t\Upsilon_1(y,S)\,dy,\\
I(t)&=I(0)+\frac{2(1-\varsigma)}{(2-\varsigma)\mathcal{Z}(\varsigma)}\Upsilon_2(t,I)+\frac{2\varsigma}{(2-\varsigma)\mathcal{Z}(\varsigma)}\int_0^t\Upsilon_2(y,I)\,dy,\\
C(t)&=C(0)+\frac{2(1-\varsigma)}{(2-\varsigma)\mathcal{Z}(\varsigma)}\Upsilon_3(t,C)+\frac{2\varsigma}{(2-\varsigma)\mathcal{Z}(\varsigma)}\int_0^t\Upsilon_3(y,C)\,dy,\\
T(t)&=T(0)+\frac{2(1-\varsigma)}{(2-\varsigma)\mathcal{Z}(\varsigma)}\Upsilon_4(t,T)+\frac{2\varsigma}{(2-\varsigma)\mathcal{Z}(\varsigma)}\int_0^t\Upsilon_4(y,T)\,dy,\\
A(t)&=A(0)+\frac{2(1-\varsigma)}{(2-\varsigma)\mathcal{Z}(\varsigma)}\Upsilon_5(t,A)+\frac{2\varsigma}{(2-\varsigma)\mathcal{Z}(\varsigma)}\int_0^t\Upsilon_5(y,A)\,dy.
\end{aligned}\tag{23}$$

where the initial data are $S^0(t)=S(0), I^0(t)=I(0), C^0(t)=C(0), T^0(t)=T(0), A^0(t)=A(0)$.

The corresponding iterative scheme is

$$\begin{aligned}
S_n(t)&=\frac{2(1-\varsigma)}{(2-\varsigma)\mathcal{Z}(\varsigma)}\Upsilon_1\left(t,S_{n-1}\right)+\frac{2\varsigma}{(2-\varsigma)\mathcal{Z}(\varsigma)}\int_0^t\Upsilon_1\left(y,S_{n-1}\right)dy,\\
I_n(t)&=\frac{2(1-\varsigma)}{(2-\varsigma)\mathcal{Z}(\varsigma)}\Upsilon_1\left(t,I_{n-1}\right)+\frac{2\varsigma}{(2-\varsigma)\mathcal{Z}(\varsigma)}\int_0^t\Upsilon_1\left(y,I_{n-1}\right)dy,\\
C_n(t)&=\frac{2(1-\varsigma)}{(2-\varsigma)\mathcal{Z}(\varsigma)}\Upsilon_1\left(t,C_{n-1}\right)+\frac{2\varsigma}{(2-\varsigma)\mathcal{Z}(\varsigma)}\int_0^t\Upsilon_1\left(y,C_{n-1}\right)dy,\\
T_n(t)&=\frac{2(1-\varsigma)}{(2-\varsigma)\mathcal{Z}(\varsigma)}\Upsilon_1\left(t,T_{n-1}\right)+\frac{2\varsigma}{(2-\varsigma)\mathcal{Z}(\varsigma)}\int_0^t\Upsilon_1\left(y,T_{n-1}\right)dy,\\
A_n(t)&=\frac{2(1-\varsigma)}{(2-\varsigma)\mathcal{Z}(\varsigma)}\Upsilon_1\left(t,A_{n-1}\right)+\frac{2\varsigma}{(2-\varsigma)\mathcal{Z}(\varsigma)}\int_0^t\Upsilon_1\left(y,A_{n-1}\right)dy,
\end{aligned}\tag{24}$$

and analogous formulas hold for I_n, C_n, T_n, A_n. Because the Lipschitz constants μ_i satisfy $\mu_i<1$, the Banach fixed point theorem guarantees the existence of a unique solution for the considered system with CF derivative.

The difference terms are derived as:

$$\begin{aligned}
K_{1n}(t)&=S_n(t)-S_{n-1}(t)=\frac{2(1-\varsigma)}{(2-\varsigma)\mathcal{Z}(\varsigma)}\left(\Upsilon_1(t,S_{n-1})-\Upsilon_1(t,S_{n-2})\right)\\
&\quad+\frac{2\varsigma}{(2-\varsigma)\mathcal{Z}(\varsigma)}\int_0^t\left(\Upsilon_1(y,S_{n-1})-\Upsilon_1(y,S_{n-2})\right)dy,\\
K_{2n}(t)&=I_n(t)-I_{n-1}(t)=\frac{2(1-\varsigma)}{(2-\varsigma)\mathcal{Z}(\varsigma)}\Upsilon_2\left((t,I_{n-1})-\Upsilon_2(t,I_{n-2})\right)\\
&\quad+\frac{2\varsigma}{(2-\varsigma)\mathcal{Z}(\varsigma)}\int_0^t\left(\Upsilon_2(y,I_{n-1})-\Upsilon_2(y,I_{n-2})\right)dy,\\
K_{3n}(t)&=C_n(t)-C_{n-1}(t)=\frac{2(1-\varsigma)}{(2-\varsigma)\mathcal{Z}(\varsigma)}\left(\Upsilon_3(t,C_{n-1})-\Upsilon_3(t,C_{n-2})\right)\\
&\quad+\frac{2\varsigma}{(2-\varsigma)\mathcal{Z}(\varsigma)}\int_0^t\left(\Upsilon_3(y,C_{n-1})-\Upsilon_3(y,C_{n-2})\right)dy,\\
K_{4n}(t)&=T_n(t)-T_{n-1}(t)=\frac{2(1-\varsigma)}{(2-\varsigma)\mathcal{Z}(\varsigma)}\left(\Upsilon_4(t,T_{n-1})-\Upsilon_4(t,T_{n-2})\right)\\
&\quad+\frac{2\varsigma}{(2-\varsigma)\mathcal{Z}(\varsigma)}\int_0^t\left(\Upsilon_4(y,T_{n-1})-\Upsilon_4(y,T_{n-2})\right)dy,\\
K_{5n}(t)&=A_n(t)-A_{n-1}(t)=\frac{2(1-\varsigma)}{(2-\varsigma)\mathcal{Z}(\varsigma)}\left(\Upsilon_5(t,A_{n-1})-\Upsilon_5(t,A_{n-2})\right)\\
&\quad+\frac{2\varsigma}{(2-\varsigma)\mathcal{Z}(\varsigma)}\int_0^t\left(\Upsilon_5(y,A_{n-1})-\Upsilon_5(y,A_{n-2})\right)dy.
\end{aligned}$$

Then we can write that

$$\begin{aligned}
S_n(t)&=\sum_{i=1}^n K_{1i}(t),\quad I_n(t)=\sum_{i=1}^n K_{2i}(t),\quad C_n(t)=\sum_{i=1}^n K_{3i}(t),\\
T_n(t)&=\sum_{i=1}^n K_{4i}(t),\quad A_n(t)=\sum_{i=1}^n K_{5i}(t),
\end{aligned}$$

and using the Lipschitz property of Υ_1, we obtain

$$\begin{aligned}
\|K_{1n}(t)\|&=\|S_n(t)-S_{n-1}(t)\|\\
&\le\frac{2(1-\varsigma)}{(2-\varsigma)\mathcal{Z}(\varsigma)}\left(\Upsilon_1(t,S_{n-1})-\Upsilon_1(t,S_{n-2})\right)\\
&\quad+\frac{2\varsigma}{(2-\varsigma)\mathcal{Z}(\varsigma)}\int_0^t\left(\Upsilon_1(y,S_{n-1})-\Upsilon_1(y,S_{n-2})\right)dy\\
&\le\frac{2(1-\varsigma)}{(2-\varsigma)\mathcal{Z}(\varsigma)}\mu_1\|S_{n-1}(t)-S_{n-2}(t)\|\\
&\quad+\frac{2\varsigma}{(2-\varsigma)\mathcal{Z}(\varsigma)}\mu_1\int_0^t\|S_{n-1}(y)-S_{n-2}(y)\|dy,
\end{aligned}\tag{25}$$

where $\mu_1<1$ is the Lipschitz constant from (21). Analogous estimates hold for K_{2n}, K_{3n}, K_{4n}, and K_{5n}:

$$\|K_{2n}(t)\|\le\frac{2(1-\varsigma)}{(2-\varsigma)\mathcal{U}(\varsigma)}\mu_2\|I_{n-1}(t)-I_{n-2}(t)\|$$

$$+\frac{2\varsigma}{(2-\varsigma)\mathcal{Z}(\varsigma)}\mu_2\int_0^t\|I_{n-1}(y)-I_{n-2}(y)\|dy,$$

$$\|K_{3n}(t)\|\le\frac{2(1-\varsigma)}{(2-\varsigma)\mathcal{U}(\varsigma)}\mu_3\|C_{n-1}(t)-C_{n-2}(t)\|+\frac{2\varsigma}{(2-\varsigma)\mathcal{Z}(\varsigma)}\mu_3\int_0^t\|C_{n-1}(y)-C_{n-2}(y)\|dy,$$

$$\|K_{4n}(t)\|\le\frac{2(1-\varsigma)}{(2-\varsigma)\mathcal{U}(\varsigma)}\mu_4\|T_{n-1}(t)-T_{n-2}(t)\|+\frac{2\varsigma}{(2-\varsigma)\mathcal{Z}(\varsigma)}\mu_4\int_0^t\|T_{n-1}(y)-T_{n-2}(y)\|dy, \tag{26}$$

$$\|K_{5n}(t)\|\le\frac{2(1-\varsigma)}{(2-\varsigma)\mathcal{U}(\varsigma)}\mu_5\|A_{n-1}(t)-A_{n-2}(t)\|+\frac{2\varsigma}{(2-\varsigma)\mathcal{Z}(\varsigma)}\mu_5\int_0^t\|A_{n-1}(y)-A_{n-2}(y)\|dy, \tag{27}$$

Hence, the model (11) has a solution □

Theorem 3.2. *The HIV model (11) with the CF operator admits a unique solution if*

$$\left(\frac{2(1-\varsigma)}{(2-\varsigma)\mathcal{Z}(\varsigma)}+\frac{2\varsigma t}{(2-\varsigma)\mathcal{Z}(\varsigma)}\right)\mu_i\le 1,\quad i=1,2,3,4,5,$$

where μ_i are the Lipschitz constants of the nonlinear functions Υ_i.

Proof. Suppose, contrary to our claim, that there is another solution

$$S^*(t),\ I^*(t),\ C^*(t),\ T^*(t),\ A^*(t)$$

having the same initial values. Then, by the integral form of the CF derivative,

$$S^*(t)=S(0)+\frac{2(1-\varsigma)}{(2-\varsigma)\mathcal{Z}(\varsigma)}\Upsilon_1(t,S^*)+\frac{2\varsigma}{(2-\varsigma)\mathcal{Z}(\varsigma)}\int_0^t\Upsilon_1(y,S^*)\,dy,$$

$$I^*(t)=I(0)+\frac{2(1-\varsigma)}{(2-\varsigma)\mathcal{Z}(\varsigma)}\Upsilon_2(t,I^*)+\frac{2\varsigma}{(2-\varsigma)\mathcal{Z}(\varsigma)}\int_0^t\Upsilon_2(y,I^*)\,dy,$$

$$C^*(t)=C(0)+\frac{2(1-\varsigma)}{(2-\varsigma)\mathcal{Z}(\varsigma)}\Upsilon_3(t,C^*)+\frac{2\varsigma}{(2-\varsigma)\mathcal{Z}(\varsigma)}\int_0^t\Upsilon_3(y,C^*)\,dy,$$

$$T^*(t)=T(0)+\frac{2(1-\varsigma)}{(2-\varsigma)\mathcal{Z}(\varsigma)}\Upsilon_4(t,T^*)+\frac{2\varsigma}{(2-\varsigma)\mathcal{Z}(\varsigma)}\int_0^t\Upsilon_4(y,T^*)\,dy,$$

$$A^*(t)=A(0)+\frac{2(1-\varsigma)}{(2-\varsigma)\mathcal{Z}(\varsigma)}\Upsilon_5(t,A^*)+\frac{2\varsigma}{(2-\varsigma)\mathcal{Z}(\varsigma)}\int_0^t\Upsilon_5(y,A^*)\,dy.$$

Subtracting the two solutions and using the Lipschitz property

$$\begin{aligned}\|S-S^*\|&=\left\|\frac{2(1-\varsigma)}{(2-\varsigma)\mathcal{U}(\varsigma)}\left(\Upsilon_1(t,S)-\Upsilon_1(t,S^*)\right)+\frac{2\varsigma}{(2-\varsigma)\mathcal{Z}(\varsigma)}\int_0^t\left(\Upsilon_1(y,S)-\Upsilon_1(y,S^*)\right)dy\right\|\\&\le\frac{2(1-\varsigma)}{(2-\varsigma)\mathcal{Z}(\varsigma)}\|\Upsilon_1(t,S)-\Upsilon_1(t,S^*)\|+\frac{2\varsigma}{(2-\varsigma)\mathcal{Z}(\varsigma)}\int_0^t\|\Upsilon_1(y,S)-\Upsilon_1(y,S^*)\|\,dy\\&\le\frac{2(1-\varsigma)}{(2-\varsigma)\mathcal{Z}(\varsigma)}\mu_1\|S-S^*\|+\frac{2\varsigma}{(2-\varsigma)\mathcal{Z}(\varsigma)}\mu_1\int_0^t\|S-S^*\|\,dy\\&=\left(\frac{2(1-\varsigma)}{(2-\varsigma)\mathcal{Z}(\varsigma)}\mu_1+\frac{2\varsigma}{(2-\varsigma)\mathcal{Z}(\varsigma)}\mu_1 t\right)\|S-S^*\|.\end{aligned}$$

Thus,

$$\left(1-\left(\frac{2(1-\varsigma)}{(2-\varsigma)\mathcal{Z}(\varsigma)}+\frac{2\varsigma}{(2-\varsigma)\mathcal{Z}(\varsigma)}t\right)\mu_1\right)\|S-S^*\|\le 0.$$

As a result, $\|S-S^*\|=0\implies S=S^*$. In a similar manner, we can demonstrate

$$I=I^*,\quad C=C^*,\quad T=T^*,\quad A=A^*.$$

Hence, the model (11) has a unique solution. □

3.1. UH stability

The concept originates from Ulam of question on the stability of group homomorphisms, which was answered by Hyers through the study of additive mappings on Banach spaces using the contraction mapping theorem [46,52,53]. In differential equations, UH stability ensures that approximate solutions remain close to exact ones under small perturbations. Establishing UH stability therefore complements existence and uniqueness by confirming that the system under CF derivative is robust and well-posed, even when the dynamics or numerical approximations are slightly altered. To establish the UH stability of the model (11) under the CF derivative. The HIV model is said to be UH stable if, for any $\epsilon_i>0$ $(i=1,\dots,5)$, there exists a true solution $(S^*(t),I^*(t),C^*(t),T^*(t),A^*(t))$ such that the approximate solutions (S,I,C,T,A) satisfy

$$\|S-S^*\|\le\eta_1\epsilon_1,\quad \|I-I^*\|\le\eta_2\epsilon_2,\quad \|C-C^*\|\le\eta_3\epsilon_3,\quad \|T-T^*\|\le\eta_4\epsilon_4,\quad \|A-A^*\|\le\eta_5\epsilon_5,$$

for some bounded constants $\eta_i>0$.

Remark 3.1. If S satisfies

$$\left\|{}^{CF}D^{\varsigma}S(t)-\Upsilon_1(t,S)\right\|\le\epsilon_1,$$

then there exists a continuous perturbation $h_1(t)$ with $|h_1(t)|<\epsilon_1$ such that

$${}^{CF}D^{\varsigma}S(t)=\Upsilon_1(t,S)+h_1(t).$$

Similar perturbations $h_i(t)$ exist for I,C,T, and A.

Theorem 3.3. *Assume the nonlinearities Υ_i $(i=1,\dots,5)$ satisfy a Lipschitz condition with constants μ_i. Then, the model (11) is UH stable provided*

$$\left(\frac{2(1-\varsigma)}{(2-\varsigma)\mathcal{M}(\varsigma)}+\frac{2\varsigma t}{(2-\varsigma)\mathcal{M}(\varsigma)}\right)\mu_i<1.$$

Proof. Suppose S is an approximate solution with perturbation h_1, so that

$${}^{CF}D^{\varsigma}S(t)=\Upsilon_1(t,S)+h_1(t).$$

Then

$$S(t)=S(0)+\frac{2(1-\varsigma)}{(2-\varsigma)\mathcal{Z}(\varsigma)}\Upsilon_1(t,S)+\frac{2\varsigma}{(2-\varsigma)\mathcal{Z}(\varsigma)}\int_0^t\Upsilon_1(y,S(y))\,dy+\frac{2(1-\varsigma)}{(2-\varsigma)\mathcal{Z}(\varsigma)}h_1(t)+\frac{2\varsigma}{(2-\varsigma)\mathcal{Z}(\varsigma)}\int_0^t h_1(y)\,dy.$$

The exact solution $S^*(t)$ satisfies the same relation without the perturbation terms. Taking the difference yields

$$|S(t)-S^*(t)|\le\left(\frac{2(1-\varsigma)}{(2-\varsigma)\mathcal{Z}(\varsigma)}+\frac{2\varsigma}{(2-\varsigma)\mathcal{Z}(\varsigma)}\right)\mu_1\|S-S^*\|+\left(\frac{2(1-\varsigma)}{(2-\varsigma)\mathcal{Z}(\varsigma)}+\frac{2\varsigma}{(2-\varsigma)\mathcal{Z}(\varsigma)}\right)\epsilon_1.$$

Hence,

$$\|S-S^*\|\le\eta_1\epsilon_1,\quad \eta_1=\frac{\left(\frac{2(1-\varsigma)}{(2-\varsigma)\mathcal{Z}(\varsigma)}+\frac{2\varsigma}{(2-\varsigma)\mathcal{Z}(\varsigma)}\right)}{1-\left(\frac{2(1-\varsigma)}{(2-\varsigma)\mathcal{Z}(\varsigma)}+\frac{2\varsigma}{(2-\varsigma)\mathcal{Z}(\varsigma)}\right)\mu_1}.$$

Analogous estimates hold for V,E,I, and R, yielding

$$\|I-I^*\|\le\eta_2\epsilon_2,\quad \|C-C^*\|\le\eta_3\epsilon_3,\quad \|T-T^*\|\le\eta_4\epsilon_4,\quad \|A-A^*\|\le\eta_5\epsilon_5.$$

Thus, the model (11) is UH stable. □

4. Local and global stability

This section describes local and global stability analysis.

Theorem 4.1. *The infection-free equilibrium point E_0 of model (11) is locally asymptotically stable for $R_0 < 1$, and unstable when $R_0 > 1$.*

Proof. Local stability of the infection-free equilibrium E_0 follows from the spectrum of the Jacobian at E_0, given by:

$$\mathcal{J}_{E_0} = \begin{pmatrix} \lambda+\mu & 0 & 0 & 0 & 0 \\ 0 & \lambda+\Theta_1 & 0 & 0 & 0 \\ 0 & -\gamma_{IC} & \lambda+\Theta_2 & -\rho & 0 \\ 0 & -\tau_I & -\tau_C & \lambda+\Theta_3 & -\tau_A \\ 0 & 0 & -\gamma_{CA} & -\theta_T & \lambda+\Theta_4 \end{pmatrix} \tag{28}$$

where,

$$\Theta_1 = \mu+\gamma_{IC}+\tau_I+\alpha_I,$$
$$\Theta_2 = \mu+\gamma_{CA}+\tau_C+\alpha_C,$$
$$\Theta_3 = \mu+\rho+\theta_T,$$
$$\Theta_4 = \mu+\delta+\tau_A+\alpha_A.$$

At the infection–free equilibrium E_0, the characteristic equation is given by

$$P(\lambda) = \left| \lambda I - J_{E_0} \right|,$$

which, as defined in Eq. (28), follows directly from the Jacobian matrix evaluated at E_0.

$$P = det\begin{pmatrix} \lambda+\mu & 0 & 0 & 0 & 0 \\ 0 & \lambda+\Theta_1 & 0 & 0 & 0 \\ 0 & -\gamma_{IC} & \lambda+\Theta_2 & -\rho & 0 \\ 0 & -\tau_I & -\tau_C & \lambda+\Theta_3 & -\tau_A \\ 0 & 0 & -\gamma_{CA} & -\theta_T & \lambda+\Theta_4 \end{pmatrix}$$

The associated characteristics equation of $P(\lambda+\mu)(\lambda+\Theta_1)(\lambda^3+c_1\lambda^2+c_2\lambda+c_3)$,

$$c_1 = \mu+\Theta_1+\Theta_2+\Theta_3+\Theta_4,$$
$$c_2 = \mu(\Theta_1+\Theta_2+\Theta_3+\Theta_4)+\Theta_1(\Theta_2+\Theta_3)+\Theta_4(\Theta_1+\Theta_2) + \Theta_3(\Theta_2+\Theta_4)-(\rho\tau_C+\tau_A\theta_T),$$
$$c_3 = +\Theta_2\Theta_4(\mu+\Theta_1)+\Theta_3\Theta_4(\mu+\Theta_2)+\Theta_1\Theta_2(\mu+\Theta_3)+\Theta_1\Theta_3(\mu+\Theta_4) + \mu(\Theta_1\Theta_4+\Theta_2\Theta_3) - \rho\tau_C(\Theta_1-\Theta_4)-\tau_A\theta_T(\Theta_1-\Theta_2)-\mu\tau_A\theta_T-\rho(\tau_A\gamma_{AC}+\mu\tau_C),$$
$$c_4 = \mu\Theta_3\Theta_4(\Theta_1+\Theta_2)-\rho\Theta_1(\tau_A\gamma_{AC}+\mu\tau_C)-\Theta_1\tau_A\theta_T(\mu+\Theta_2) + \Theta_1\Theta_2\Theta_3(\mu+\Theta_4) - \mu(\rho\tau_A\gamma_{AC}+\rho\Theta_4\tau_C+\Theta_2\tau_A\theta_T)+\Theta_1\Theta_4(\mu\Theta_2-\rho\tau_C),$$
$$c_5 = \mu(\Theta_1\Theta_2\Theta_3\Theta_4-\rho\Theta_1\tau_A\gamma_{AC}-\Theta_1\Theta_2\tau_A\theta_T-\rho\Theta_1\Theta_4\tau_C).$$

According to the Routh–Hurwitz stability criterion, the equilibrium E_0 is locally asymptotically stable if and only if all the Hurwitz determinants $H_i > 0$ *where* $i = 1,2,3,4,5$.

$$H_1 = c_1 > 0, \quad H_2 = \begin{vmatrix} c_1 & 1 \\ c_3 & c_2 \end{vmatrix} > 0, \quad H_3 = \begin{vmatrix} c_1 & 1 & 0 \\ c_3 & c_2 & c_1 \\ c_5 & c_4 & c_3 \end{vmatrix} > 0,$$

$$H_4 = \begin{vmatrix} c_1 & 1 & 0 & 0 \\ c_3 & c_2 & c_1 & 1 \\ c_5 & c_4 & c_3 & c_2 \\ 0 & 0 & c_5 & c_4 \end{vmatrix} > 0, H_5 = c_5H_4 > 0.$$

Hence, Hurwitz determinants are positive, then all the eigenvalues of $J(E_0)$ have negative real parts, ensuring that the equilibrium point E_0 is locally asymptotically stable.

Theorem 4.2. *The persistent-infection equilibrium point, E^* is globally asymptotically stable when $R_0 > 1$, and unstable otherwise.*

Proof. Consider the nonlinear Lyapunov function defined as:

$$\begin{aligned} {}^{CF}D_t^{\varsigma}L = {} & l_1\left(1-\frac{S^*}{S}\right){}^{CF}S_t^{\varsigma} + l_2\left(1-\frac{I^*}{I}\right){}^{CF}I_t^{\varsigma} \\ & + l_3\left(1-\frac{C^*}{C}\right){}^{CF}C_t^{\varsigma} + l_4\left(1-\frac{T^*}{T}\right){}^{CF}T_t^{\varsigma} + l_5\left(1-\frac{A^*}{A}\right){}^{CF}A_t^{\varsigma} \end{aligned} \tag{29}$$

Using system (11) in Eq. (29), the resulting expression is

$$\begin{aligned} {}^{CF}D_t^{\varsigma}L = {} & l_1\left(1-\frac{S^*}{S}\right)(\Lambda-\psi S-\mu S) + l_2\left(1-\frac{I^*}{I}\right) \\ & (\psi S-(\mu+\gamma_{IC}+\tau_I+\alpha_I)I) + l_3\left(1-\frac{C^*}{C}\right) \\ & (\gamma_{IC}I-(\mu+\gamma_{CA}+\tau_C+\alpha_C)C+\rho T) \\ & + l_4\left(1-\frac{T^*}{T}\right)(\tau_I I+\tau_C C+\tau_A A-(\mu+\rho+\theta_T)T)) \\ & + l_5\left(1-\frac{A^*}{A}\right)(\gamma_{CA}C+\theta_T T-(\mu+\delta+\tau_A+\alpha_A)A). \end{aligned} \tag{30}$$

Noting that E^* is an equilibrium of model (11), we observe that

$$\begin{aligned} \Lambda &= \psi^*S^*+\mu S^*, \\ \mu+\gamma_{IC}+\tau_I+\alpha_I &= \psi^*\frac{S^*}{I^*}, \\ \mu+\gamma_{CA}+\tau_C+\alpha_C &= \frac{\gamma_{IC}I^*+\rho T^*}{C}, \\ \mu+\rho+\theta_T &= \frac{\tau_I I^*+\tau_C C^*+\tau_A A^*}{T}, \\ \mu+\delta+\tau_A+\alpha_A &= \frac{\gamma_{CA}C^*+\theta_T T^*}{A^*}. \end{aligned} \tag{31}$$

Substituting Eq. (31) into Eq. (30) yields:

$$\begin{aligned} {}^{CF}D_t^{\varsigma}L = {} & l_1(\psi^*S^*+\mu S^*)\left(\frac{S^*}{S}-\frac{S}{S^*}\right) + l_2\psi^*S^*\left(\frac{S}{S^*}-\frac{I^*}{I}-\frac{IS}{I^*S^*}+1\right) \\ & + l_3\gamma_{IC}I^*\left(\frac{I}{I^*}-\frac{C^*}{C}-\frac{I}{I^*}\frac{C}{C^*}+1\right) \\ & + l_3\rho T^*\left(\frac{C}{C^*}\frac{T}{T^*}-\frac{C^*}{C}-\frac{T}{T^*}+1\right) \\ & + \tau_I I^* l_4\left(\frac{I}{I^*}-\frac{T^*}{T}-\frac{I}{I^*}\frac{T}{T^*}+1\right) \\ & + \tau_C C^* l_4\left(\frac{C}{C^*}-\frac{T^*}{T}-\frac{C}{C^*}\frac{T}{T^*}+1\right) \\ & + \tau_A A^* l_4\left(\frac{A}{A^*}-\frac{T^*}{T}-\frac{T}{T^*}\frac{A}{A^*}+1\right) \\ & + \gamma_{CA}C^* l_5\left(\frac{C}{C^*}-\frac{A^*}{A}-\frac{C}{C^*}\frac{A}{A^*}+1\right) \\ & + \theta_T T^* l_5\left(\frac{T}{T^*}-\frac{A^*}{A}-\frac{T}{T^*}\frac{A}{A^*}+1\right). \end{aligned} \tag{32}$$

Through algebraic manipulation, Eq. (32) reduces to:

$$\begin{aligned} {}^{CF}D_t^{\varsigma}L = {} & (\psi^*S^*+\mu S^*)\left(2-\frac{S}{S^*}-\frac{S^*}{S}\right) \\ & + \left(\gamma_{IC}I^*+\frac{\rho\tau_I I^*T^*}{\tau_C C^*}\right)\left(2-\frac{I}{I^*}-\frac{I^*}{I}\right) \\ & + \left(\frac{\gamma_{CA}C^*\rho}{\theta_T}+\frac{\tau_C C^*\rho T^*}{\tau_C C^*}\right)\left(2-\frac{C^*}{C}-\frac{C}{C^*}\right) \end{aligned} \tag{33}$$

$$+\left(2-\frac{T^*}{T}-\frac{T}{T^*}\right)+\left(\frac{\gamma_{CA}C^*\rho}{\theta_T}+\frac{\theta_T T^*\rho}{\theta_T}\right)$$
$$\left(3-\frac{T^*A^*}{TA}-\frac{T}{T^*}-\frac{A}{A^*}\right)+\left(\frac{\gamma_{CA}C^*\rho}{\theta_T}\right)$$
$$\left(3-\frac{C^*A^*}{CA}+\frac{C}{C^*}+\frac{A}{A^*}\right).$$

Through the use of the arithmetic–geometric mean inequality, the inequalities in Eq. (33) are established as follows:

$$\begin{aligned}
&2-\frac{T^*}{T}-\frac{T}{T^*}\le 0,\\
&2-\frac{I}{I^*}-\frac{I^*}{I}\le 0,\\
&2-\frac{C^*}{C}-\frac{C}{C^*}\le 0,\\
&2-\frac{T^*}{T}-\frac{T}{T^*}\le 0,
\end{aligned}\tag{34}$$

$$\begin{aligned}
&3-\frac{T^*A^*}{TA}-\frac{T}{T^*}-\frac{A}{A^*}\le 0,\\
&3-\frac{C^*A^*}{CA}+\frac{C}{C^*}+\frac{A}{A^*}\le 0.
\end{aligned}$$

Thus, ${}^{CF}D_t^{\varsigma}L\le 0$ for $R_0>1$, and ${}^{CF}D_t^{\varsigma}L=0$ at $S=S^*, I=I^*, C=C^*, T=T^*, A=A^*$. LaSalle's invariance principle implies that when $R_0>1$, the system approaches the persistent-infection equilibrium in Ω from any initial condition, indicating global asymptotic stability.

5. Numerical scheme

For the numerical simulations, we employed the Adams–Bashforth scheme adapted to the CF fractional derivative, and convergence is outlined in [54]. For the kernels Υ_i $(i=1,2,3,4)$, the following integral system is obtained:

$$S(t)-S(0)=\frac{1-\varsigma}{\mathcal{Z}(\varsigma)}\Upsilon_1(t,S(t))+\frac{\varsigma}{\mathcal{Z}(\varsigma)}\int_0^t\Upsilon_1(\tau,S(\tau))d\tau,$$

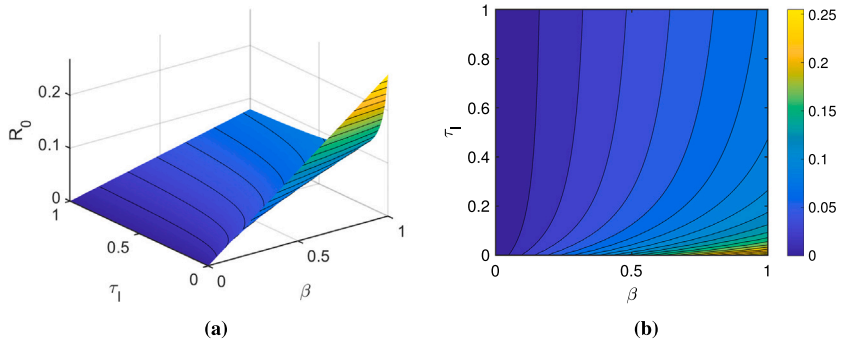

Fig. 3. R_0 as a function of the baseline transmission rate β and the treatment initiation rate for acute infection τ_I.

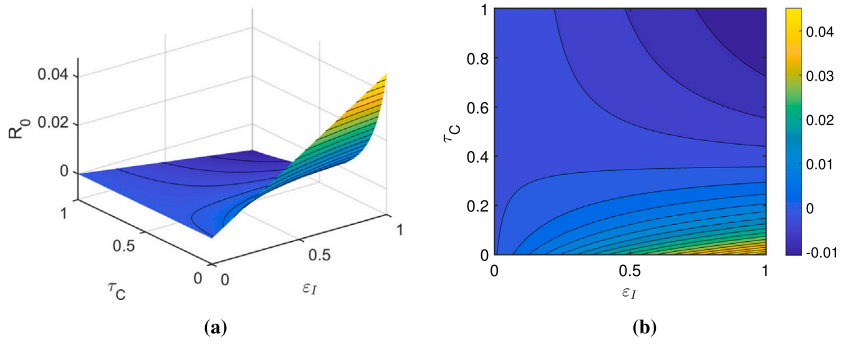

Fig. 4. R_0 as a function of the relative infectiousness of the acute class ϵ_I and the treatment initiation rate for chronic infection τ_C.

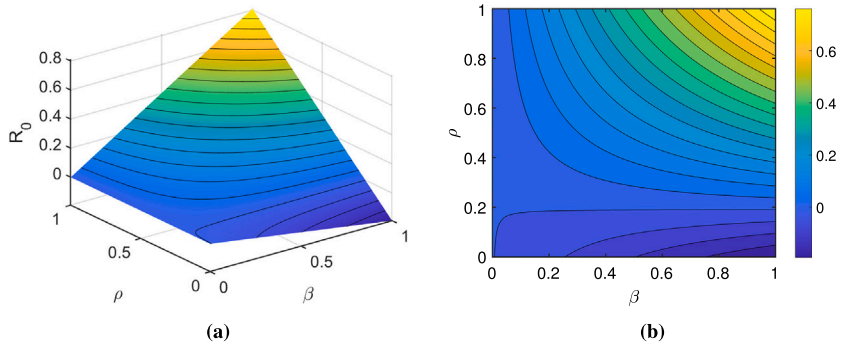

Fig. 5. R_0 as a function of the baseline transmission rate β and the ART dropout rate ρ.

$$
\begin{aligned}
I(t) - I(0) &= \frac{1-\varsigma}{\mathcal{Z}(\varsigma)}\Upsilon_2(t, I(t)) + \frac{\varsigma}{\mathcal{Z}(\varsigma)}\int_0^t \Upsilon_2(\tau, I(\tau))\, d\tau,\\
C(t) - C(0) &= \frac{1-\varsigma}{\mathcal{Z}(\varsigma)}\Upsilon_3(t, C(t)) + \frac{\varsigma}{\mathcal{Z}(\varsigma)}\int_0^t \Upsilon_3(\tau, C(\tau))\, d\tau,\\
T(t) - T(0) &= \frac{1-\varsigma}{\mathcal{Z}(\varsigma)}\Upsilon_4(t, T(t)) + \frac{\varsigma}{\mathcal{Z}(\varsigma)}\int_0^t \Upsilon_4(\tau, T(\tau))\, d\tau,\\
A(t) - A(0) &= \frac{1-\varsigma}{\mathcal{Z}(\varsigma)}\Upsilon_5(t, A(t)) + \frac{\varsigma}{\mathcal{Z}(\varsigma)}\int_0^t \Upsilon_5(\tau, A(\tau))\, d\tau,
\end{aligned} \tag{35}
$$

Discretizing the system (35) at $t = t_{n+1}$ yields:

$$
\begin{aligned}
S_{n+1} - S(0) &= \frac{1-\varsigma}{\mathcal{Z}(\varsigma)}\Upsilon_1(t_n, S(t_n)) + \frac{\varsigma}{\mathcal{Z}(\varsigma)}\int_0^{t_{n+1}} \Upsilon_1(t, S(t))\, dt,\\
I_{n+1} - I(0) &= \frac{1-\varsigma}{\mathcal{Z}(\varsigma)}\Upsilon_2(t_n, I(t_n)) + \frac{\varsigma}{\mathcal{Z}(\varsigma)}\int_0^{t_{n+1}} \Upsilon_2(t, I(t))\, dt,\\
C_{n+1} - C(0) &= \frac{1-\varsigma}{\mathcal{Z}(\varsigma)}\Upsilon_3(t_n, C(t_n)) + \frac{\varsigma}{\mathcal{Z}(\varsigma)}\int_0^{t_{n+1}} \Upsilon_3(t, C(t))\, dt,\\
T_{n+1} - T(0) &= \frac{1-\varsigma}{\mathcal{Z}(\varsigma)}\Upsilon_4(t_n, T(t_n)) + \frac{\varsigma}{\mathcal{Z}(\varsigma)}\int_0^{t_{n+1}} \Upsilon_4(t, T(t))\, dt,\\
A_{n+1} - A(0) &= \frac{1-\varsigma}{\mathcal{Z}(\varsigma)}\Upsilon_5(t_n, A(t_n)) + \frac{\varsigma}{\mathcal{Z}(\varsigma)}\int_0^{t_{n+1}} \Upsilon_5(t, A(t))dt,
\end{aligned} \tag{36}
$$

Similarly, for $t = t_n$, the discrete formulation is:

$$
\begin{aligned}
S_n - S(0) &= \frac{1-\varsigma}{\mathcal{Z}(\varsigma)}\Upsilon_1(t_{n-1}, S(t_{n-1})) + \frac{\varsigma}{\mathcal{Z}(\varsigma)}\int_0^{t_n} \Upsilon_1(t, S(t))\, dt,\\
I_n - I(0) &= \frac{1-\varsigma}{\mathcal{Z}(\varsigma)}\Upsilon_2(t_{n-1}, I(t_{n-1})) + \frac{\varsigma}{\mathcal{Z}(\varsigma)}\int_0^{t_n} \Upsilon_2(t, I(t))\, dt,\\
C_n - R(0) &= \frac{1-\varsigma}{\mathcal{Z}(\varsigma)}\Upsilon_3(t_{n-1}, C(t_{n-1})) + \frac{\varsigma}{\mathcal{Z}(\varsigma)}\int_0^{t_n} \Upsilon_3(t, C(t))\, dt,\\
T_n - T(0) &= \frac{1-\varsigma}{\mathcal{Z}(\varsigma)}\Upsilon_4(t_{n-1}, T(t_{n-1})) + \frac{\varsigma}{\mathcal{Z}(\varsigma)}\int_0^{t_n} \Upsilon_4(t, T(t))\, dt,\\
A_n - A(0) &= \frac{1-\varsigma}{\mathcal{Z}(\varsigma)}\Upsilon_5(t_{n-1}, A(t_{n-1})) + \frac{\varsigma}{\mathcal{Z}(\varsigma)}\int_0^{t_n} \Upsilon_5(t, A(t))\, dt.
\end{aligned} \tag{37}
$$

Subtracting (37) from (36), we obtain:

$$
\begin{aligned}
S_{n+1} - S_n &= \frac{1-\varsigma}{\mathcal{Z}(\varsigma)}\left[\Upsilon_1(t_n, S(t_n)) - \Upsilon_1(t_{n-1}, S(t_{n-1}))\right]\\
&\quad + \frac{\varsigma}{\mathcal{Z}(\varsigma)}\int_{t_n}^{t_{n+1}} \Upsilon_1(t, S(t))\, dt,\\
I_{n+1} - S_n &= \frac{1-\varsigma}{\mathcal{Z}(\varsigma)}\left[\Upsilon_2(t_n, I(t_n)) - \Upsilon_1(t_{n-1}, I(t_{n-1}))\right]\\
&\quad + \frac{\varsigma}{\mathcal{Z}(\varsigma)}\int_{t_n}^{t_{n+1}} \Upsilon_2(t, I(t))\, dt,
\end{aligned}
$$

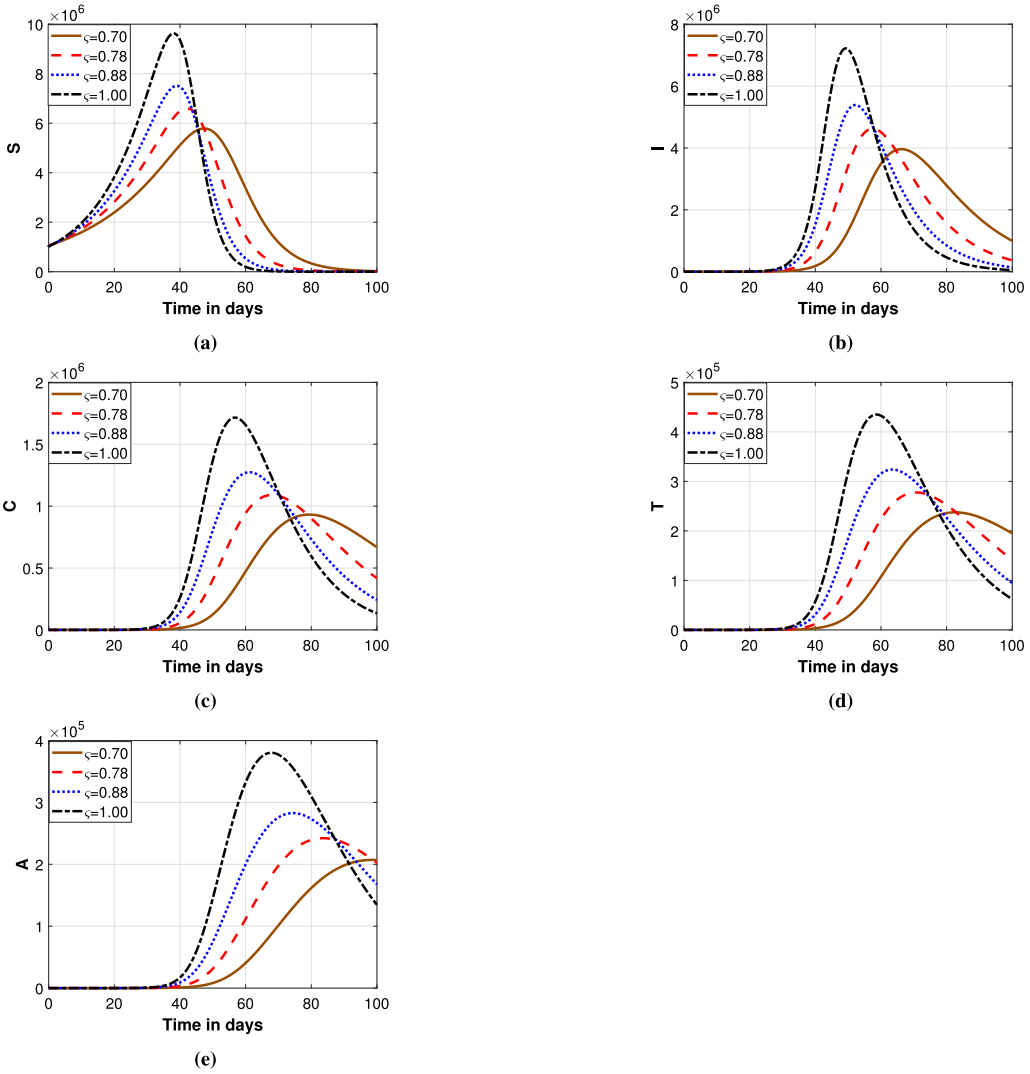

Fig. 6. Dynamics of the fractional-order model at $\varsigma = 0.70, 0.78, 0.88, 1$.

$$
\begin{aligned}
C_{n+1} - C_n &= \frac{1-\varsigma}{\mathcal{Z}(\varsigma)}\left[\Upsilon_3(t_n, C(t_n)) - \Upsilon_1(t_{n-1}, C(t_{n-1}))\right] \\
&\quad + \frac{\varsigma}{\mathcal{Z}(\varsigma)}\int_{t_n}^{t_{n+1}} \Upsilon_3(t, C(t))\, dt, \\
T_{n+1} - T_n &= \frac{1-\varsigma}{\mathcal{Z}(\varsigma)}\left[\Upsilon_4(t_n, T(t_n)) - \Upsilon_1(t_{n-1}, T(t_{n-1}))\right] \\
&\quad + \frac{\varsigma}{\mathcal{Z}(\varsigma)}\int_{t_n}^{t_{n+1}} \Upsilon_4(t, T(t))\, dt, \\
A_{n+1} - A_n &= \frac{1-\varsigma}{\mathcal{Z}(\varsigma)}\left[\Upsilon_5(t_n, A(t_n)) - \Upsilon_1(t_{n-1}, A(t_{n-1}))\right] \\
&\quad + \frac{\varsigma}{\mathcal{Z}(\varsigma)}\int_{t_n}^{t_{n+1}} \Upsilon_5(t, A(t))\, dt,
\end{aligned} \tag{38}
$$

To approximate the integral terms in Eq. (38), we apply a piecewise linear interpolation between t_n and t_{n+1}. For each kernel Υ_i, the integral is expressed as:

$$
\begin{aligned}
\int_{t_n}^{t_{n+1}} \Upsilon_1(t, S(t))\, dt &= \int_{t_n}^{t_{n+1}} \left[\frac{\Upsilon_1(t_n, S_n)(t - t_{n-1}) - \Upsilon_1(t_{n-1}, S_{n-1})(t - t_n)}{h}\right] dt \\
&= \frac{3h}{2}\Upsilon_1(t_n, S_n) - \frac{h}{2}\Upsilon_1(t_{n-1}, S_{n-1}), \\
\int_{t_n}^{t_{n+1}} \Upsilon_2(t, I(t))\, dt &= \frac{3h}{2}\Upsilon_2(t_n, I_n) - \frac{h}{2}\Upsilon_2(t_{n-1}, I_{n-1}),
\end{aligned}
$$

$$
\begin{aligned}
\int_{t_n}^{t_{n+1}} \Upsilon_3(t, C(t))\, dt &= \frac{3h}{2}\Upsilon_3(t_n, C_n) - \frac{h}{2}\Upsilon_3(t_{n-1}, C_{n-1}), \\
\int_{t_n}^{t_{n+1}} \Upsilon_4(t, T(t))\, dt &= \frac{3h}{2}\Upsilon_4(t_n, T_n) - \frac{h}{2}\Upsilon_4(t_{n-1}, T_{n-1}), \\
\int_{t_n}^{t_{n+1}} \Upsilon_5(t, A(t))\, dt &= \frac{3h}{2}\Upsilon_5(t_n, A_n) - \frac{h}{2}\Upsilon_5(t_{n-1}, A_{n-1}).
\end{aligned} \tag{39}
$$

Substituting Eq. (39) into the update equations, we obtain:

$$
\begin{aligned}
S_{n+1} - S_n &= \frac{1-\varsigma}{\mathcal{Z}(\varsigma)}\left(\Upsilon_1(t_n, S_n) - \Upsilon_1(t_{n-1}, S_{n-1})\right) + \frac{3\varsigma h}{2\mathcal{Z}(\varsigma)}\Upsilon_1(t_n, S_n) \\
&\quad - \frac{\varsigma h}{2\mathcal{Z}(\varsigma)}\Upsilon_1(t_{n-1}, S_{n-1}), \\
I_{n+1} - I_n &= \frac{1-\varsigma}{\mathcal{Z}(\varsigma)}\left(\Upsilon_2(t_n, I_n) - \Upsilon_2(t_{n-1}, I_{n-1})\right) + \frac{3\varsigma h}{2\mathcal{Z}(\varsigma)}\Upsilon_2(t_n, I_n) \\
&\quad - \frac{\varsigma h}{2\mathcal{Z}(\varsigma)}\Upsilon_2(t_{n-1}, I_{n-1}), \\
C_{n+1} - R_n &= \frac{1-\varsigma}{\mathcal{Z}(\varsigma)}\left(\Upsilon_3(t_n, C_n) - \Upsilon_3(t_{n-1}, C_{n-1})\right) + \frac{3\varsigma h}{2\mathcal{Z}(\varsigma)}\Upsilon_3(t_n, C_n) \\
&\quad - \frac{\varsigma h}{2\mathcal{Z}(\varsigma)}\Upsilon_3(t_{n-1}, C_{n-1}), \\
T_{n+1} - T_n &= \frac{1-\varsigma}{\mathcal{Z}(\varsigma)}\left(\Upsilon_4(t_n, T_n) - \Upsilon_4(t_{n-1}, T_{n-1})\right) + \frac{3\varsigma h}{2\mathcal{Z}(\varsigma)}\Upsilon_4(t_n, T_n)
\end{aligned} \tag{40}
$$

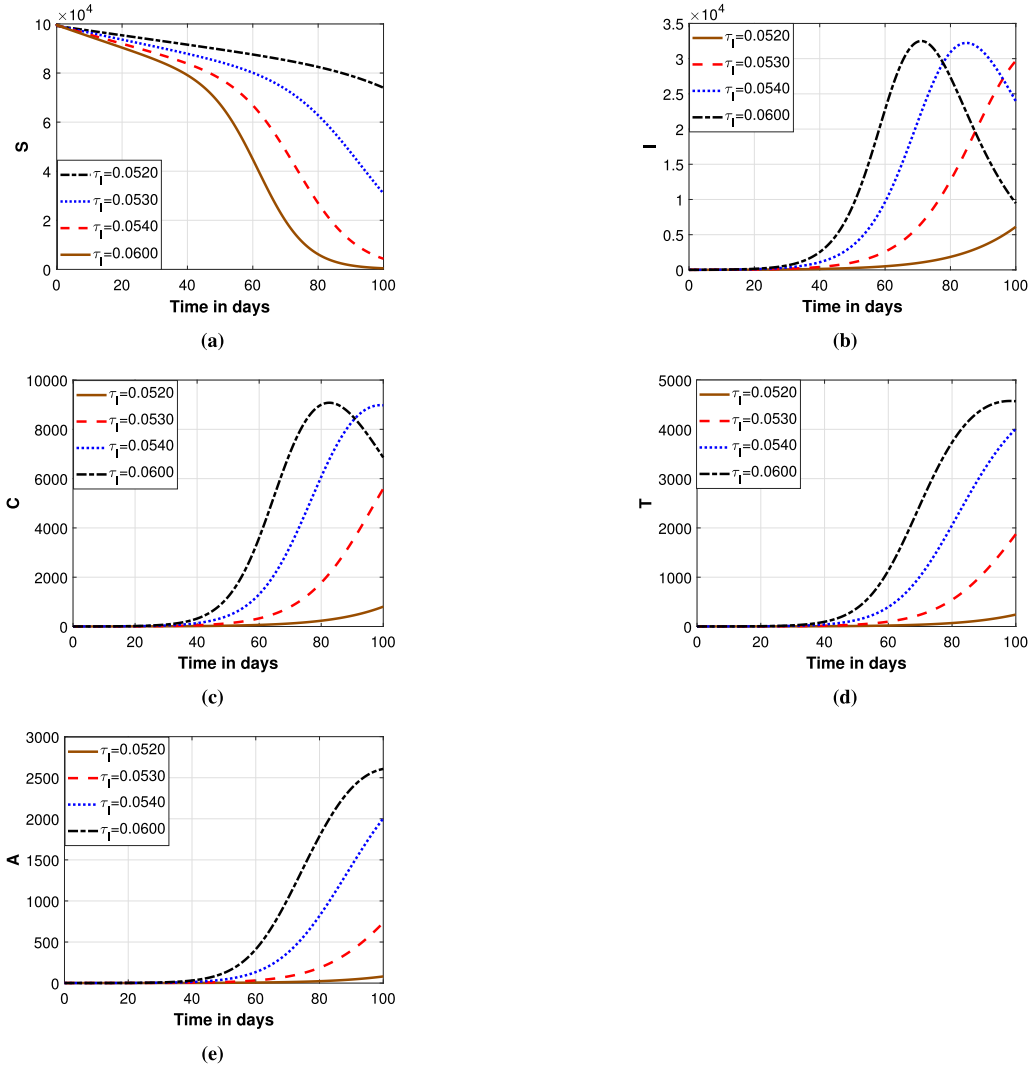

Fig. 7. Model behavior under fractional-order dynamics for τ_I, with the fractional order fixed at $\varsigma = 0.88$.

$$- \frac{\varsigma h}{2\mathcal{Z}(\varsigma)}\Upsilon_4(t_{n-1}, T_{n-1}),$$

$$A_{n+1} - A_n = \frac{1-\varsigma}{\mathcal{Z}(\varsigma)}\left(\Upsilon_5(t_n, A_n) - \Upsilon_5(t_{n-1}, A_{n-1})\right) + \frac{3\varsigma h}{2\mathcal{Z}(\varsigma)}\Upsilon_5(t_n, A_n) - \frac{\varsigma h}{2\mathcal{Z}(\varsigma)}\Upsilon_5(t_{n-1}, A_{n-1}).$$

Finally, isolating S_{n+1}, I_{n+1}, C_{n+1}, T_{n+1}, and A_{n+1} leads to the explicit update scheme:

$$\begin{aligned}
S_{n+1} &= S_n + \left(\frac{1-\varsigma}{\mathcal{Z}(\varsigma)} + \frac{3\varsigma h}{2\mathcal{Z}(\varsigma)}\right)\Upsilon_1(t_n, S_n) + \left(\frac{\varsigma h}{2\mathcal{Z}(\varsigma)} - \frac{1-\varsigma}{\mathcal{Z}(\varsigma)}\right)\Upsilon_1(t_{n-1}, S_{n-1}),\\
I_{n+1} &= I_n + \left(\frac{1-\varsigma}{\mathcal{Z}(\varsigma)} + \frac{3\varsigma h}{2\mathcal{Z}(\varsigma)}\right)\Upsilon_2(t_n, I_n) + \left(\frac{\varsigma h}{2\mathcal{Z}(\varsigma)} - \frac{1-\varsigma}{\mathcal{Z}(\varsigma)}\right)\Upsilon_2(t_{n-1}, I_{n-1}),\\
C_{n+1} &= C_n + \left(\frac{1-\varsigma}{\mathcal{Z}(\varsigma)} + \frac{3\varsigma h}{2\mathcal{Z}(\varsigma)}\right)\Upsilon_3(t_n, C_n) + \left(\frac{\varsigma h}{2\mathcal{Z}(\varsigma)} - \frac{1-\varsigma}{\mathcal{Z}(\varsigma)}\right)\Upsilon_3(t_{n-1}, C_{n-1}),\\
T_{n+1} &= T_n + \left(\frac{1-\varsigma}{\mathcal{Z}(\varsigma)} + \frac{3\varsigma h}{2\mathcal{Z}(\varsigma)}\right)\Upsilon_4(t_n, T_n) + \left(\frac{\varsigma h}{2\mathcal{Z}(\varsigma)} - \frac{1-\varsigma}{\mathcal{Z}(\varsigma)}\right)\Upsilon_4(t_{n-1}, T_{n-1}),\\
A_{n+1} &= A_n + \left(\frac{1-\varsigma}{\mathcal{Z}(\varsigma)} + \frac{3\varsigma h}{2\mathcal{Z}(\varsigma)}\right)\Upsilon_5(t_n, A_n) + \left(\frac{\varsigma h}{2\mathcal{Z}(\varsigma)} - \frac{1-\varsigma}{\mathcal{Z}(\varsigma)}\right)\Upsilon_5(t_{n-1}, A_{n-1}).
\end{aligned} \tag{41}$$

Eqs. (41) define a high-accuracy, two-step fractional discretization for the model (11). Substituting the approximations and simplifying, we obtain:

$$\begin{aligned}
S_{n+1} - S_n &= \frac{1-\varsigma}{\mathcal{Z}(\varsigma)}\left(\Upsilon_1(t_n, S_n) - \Upsilon_1(t_{n-1}, S_{n-1})\right) + \frac{3\varsigma h}{2\mathcal{Z}(\varsigma)}\Upsilon_1(t_n, S_n) - \frac{\varsigma h}{2\mathcal{Z}(\varsigma)}\Upsilon_1(t_{n-1}, S_{n-1}),\\
I_{n+1} - I_n &= \frac{1-\varsigma}{\mathcal{Z}(\varsigma)}\left(\Upsilon_2(t_n, I_n) - \Upsilon_2(t_{n-1}, I_{n-1})\right) + \frac{3\varsigma h}{2\mathcal{Z}(\varsigma)}\Upsilon_2(t_n, I_n) - \frac{\varsigma h}{2\mathcal{Z}(\varsigma)}\Upsilon_2(t_{n-1}, I_{n-1}),\\
C_{n+1} - C_n &= \frac{1-\varsigma}{\mathcal{Z}(\varsigma)}\left(\Upsilon_3(t_n, C_n) - \Upsilon_3(t_{n-1}, C_{n-1})\right) + \frac{3\varsigma h}{2\mathcal{Z}(\varsigma)}\Upsilon_3(t_n, C_n)
\end{aligned} \tag{42}$$

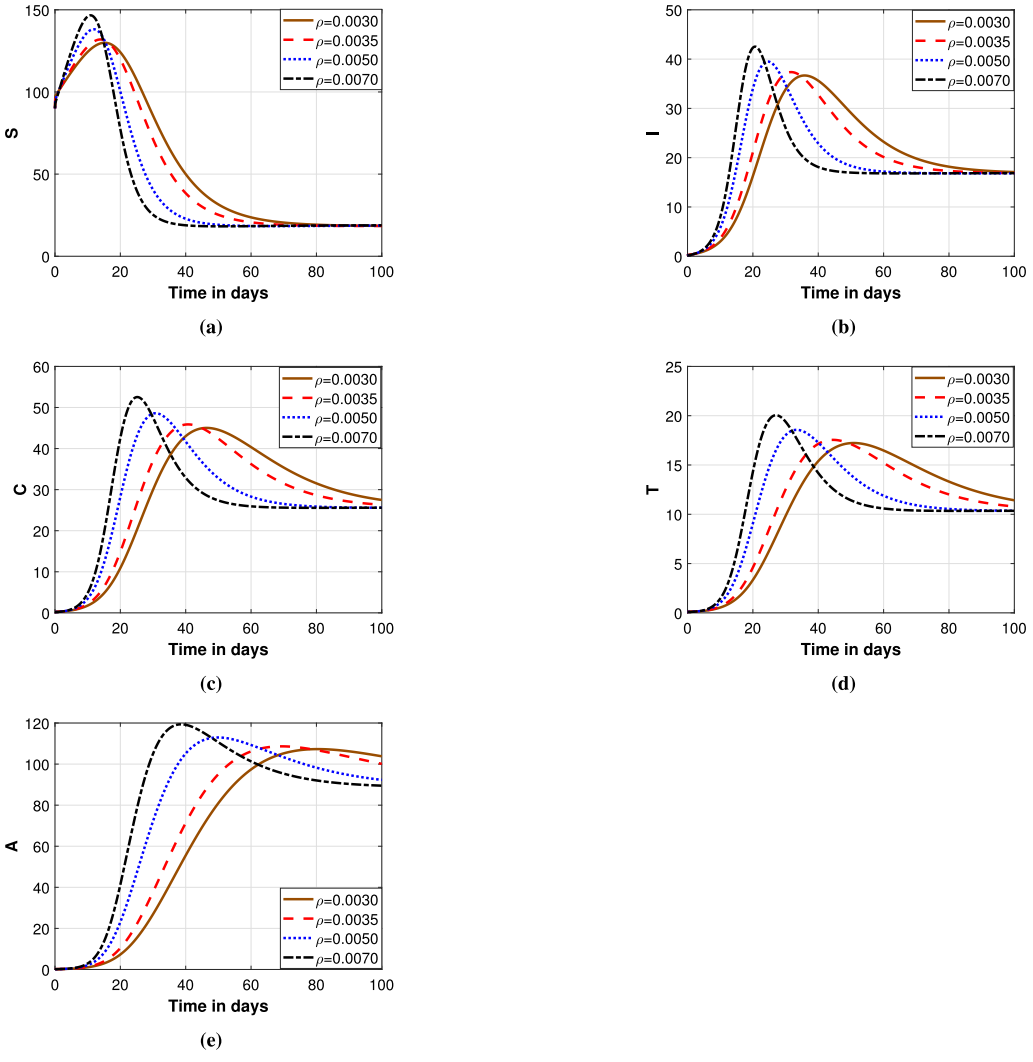

Fig. 8. Model behavior under fractional-order dynamics for ρ, with the fractional order fixed at $\varsigma = 0.88$.

$$- \frac{\varsigma h}{2\mathcal{Z}(\varsigma)}\Upsilon_3(t_{n-1}, C_{n-1}),$$

$$T_{n+1} - T_n = \frac{1-\varsigma}{\mathcal{Z}(\varsigma)}\left(\Upsilon_4(t_n, T_n) - \Upsilon_4(t_{n-1}, T_{n-1})\right) + \frac{3\varsigma h}{2\mathcal{Z}(\varsigma)}\Upsilon_4(t_n, T_n) - \frac{\varsigma h}{2\mathcal{Z}(\varsigma)}\Upsilon_4(t_{n-1}, T_{n-1}),$$

$$A_{n+1} - A_n = \frac{1-\varsigma}{\mathcal{Z}(\varsigma)}\left(\Upsilon_5(t_n, A_n) - \Upsilon_5(t_{n-1}, A_{n-1})\right) + \frac{3\varsigma h}{2\mathcal{Z}(\varsigma)}\Upsilon_5(t_n, A_n) - \frac{\varsigma h}{2\mathcal{Z}(\varsigma)}\Upsilon_5(t_{n-1}, A_{n-1}).$$

Rearranging Eq. (42), the explicit update scheme is:

$$S_{n+1} = S_n + \left(\frac{1-\varsigma}{\mathcal{Z}(\varsigma)} + \frac{3\varsigma h}{2\mathcal{Z}(\varsigma)}\right)\Upsilon_1(t_n, S_n) + \left(\frac{\varsigma h}{2\mathcal{Z}(\varsigma)} - \frac{1-\varsigma}{\mathcal{Z}(\varsigma)}\right)\Upsilon_1(t_{n-1}, S_{n-1}),$$

$$I_{n+1} = I_n + \left(\frac{1-\varsigma}{\mathcal{Z}(\varsigma)} + \frac{3\varsigma h}{2\mathcal{Z}(\varsigma)}\right)\Upsilon_2(t_n, I_n) + \left(\frac{\varsigma h}{2\mathcal{Z}(\varsigma)} - \frac{1-\varsigma}{\mathcal{Z}(\varsigma)}\right)\Upsilon_2(t_{n-1}, I_{n-1}),$$

$$C_{n+1} = C_n + \left(\frac{1-\varsigma}{\mathcal{Z}(\varsigma)} + \frac{3\varsigma h}{2\mathcal{Z}(\varsigma)}\right)\Upsilon_3(t_n, C_n) + \left(\frac{\varsigma h}{2\mathcal{Z}(\varsigma)} - \frac{1-\varsigma}{\mathcal{Z}(\varsigma)}\right)\Upsilon_3(t_{n-1}, C_{n-1}),$$

$$T_{n+1} = T_n + \left(\frac{1-\varsigma}{\mathcal{Z}(\varsigma)} + \frac{3\varsigma h}{2\mathcal{Z}(\varsigma)}\right)\Upsilon_4(t_n, T_n) + \left(\frac{\varsigma h}{2\mathcal{Z}(\varsigma)} - \frac{1-\varsigma}{\mathcal{Z}(\varsigma)}\right)\Upsilon_4(t_{n-1}, T_{n-1}),$$

$$A_{n+1} = A_n + \left(\frac{1-\varsigma}{\mathcal{Z}(\varsigma)} + \frac{3\varsigma h}{2\mathcal{Z}(\varsigma)}\right)\Upsilon_5(t_n, A_n) + \left(\frac{\varsigma h}{2\mathcal{Z}(\varsigma)} - \frac{1-\varsigma}{\mathcal{Z}(\varsigma)}\right)\Upsilon_5(t_{n-1}, A_{n-1}). \tag{43}$$

The numerical scheme satisfies:

$$S_{n+1} = S_n + \left(\frac{1-\varsigma}{\mathcal{Z}(\varsigma)} + \frac{3\varsigma h}{2\mathcal{Z}(\varsigma)}\right)\Upsilon_1(t_n, S_n) + \left(\frac{\varsigma h}{2\mathcal{Z}(\varsigma)} - \frac{1-\varsigma}{\mathcal{Z}(\varsigma)}\right)\Upsilon_1(t_{n-1}, S_{n-1}) + {}^1R_n^{\varsigma},$$

$$I_{n+1} = I_n + \left(\frac{1-\varsigma}{\mathcal{Z}(\varsigma)} + \frac{3\varsigma h}{2\mathcal{Z}(\varsigma)}\right)\Upsilon_2(t_n, I_n) + \left(\frac{\varsigma h}{2\mathcal{Z}(\varsigma)} - \frac{1-\varsigma}{\mathcal{Z}(\varsigma)}\right)\Upsilon_2(t_{n-1}, I_{n-1}) + {}^2R_n^{\varsigma},$$

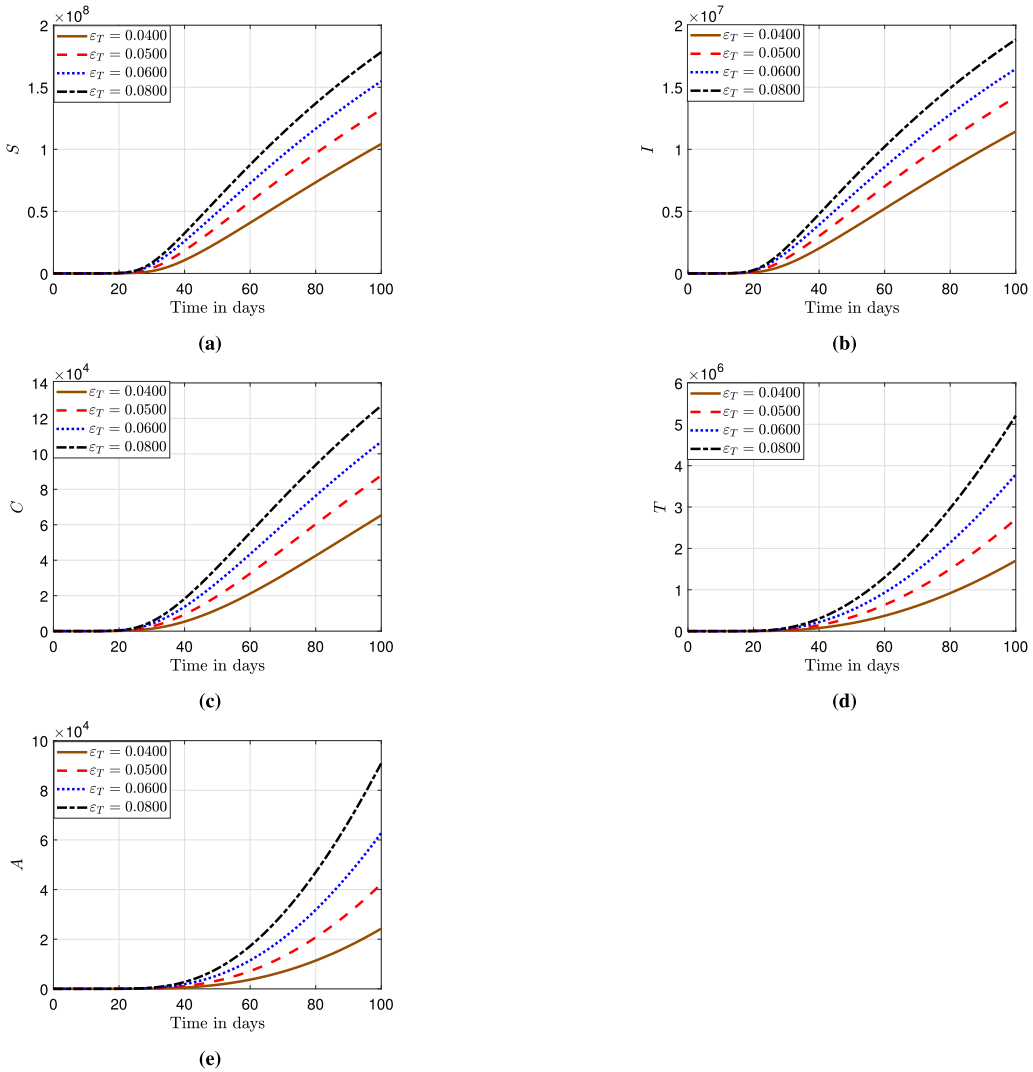

Fig. 9. Model behavior under fractional-order dynamics for ε_T, with the fractional order fixed at $\varsigma = 0.88$.

$$
\begin{aligned}
C_{n+1} &= R_n + \left(\frac{1-\varsigma}{\mathcal{Z}(\varsigma)} + \frac{3\varsigma h}{2\mathcal{Z}(\varsigma)}\right)\Upsilon_3(t_n, C_n) \\
&\quad + \left(\frac{\varsigma h}{2\mathcal{Z}(\varsigma)} - \frac{1-\varsigma}{\mathcal{Z}(\varsigma)}\right)\Upsilon_3(t_{n-1}, C_{n-1}) + {}^3R_n^{\varsigma}, \\
T_{n+1} &= T_n + \left(\frac{1-\varsigma}{\mathcal{Z}(\varsigma)} + \frac{3\varsigma h}{2\mathcal{Z}(\varsigma)}\right)\Upsilon_4(t_n, T_n) \\
&\quad + \left(\frac{\varsigma h}{2\mathcal{Z}(\varsigma)} - \frac{1-\varsigma}{\mathcal{Z}(\varsigma)}\right)\Upsilon_4(t_{n-1}, T_{n-1}) + {}^4R_n^{\varsigma}, \\
A_{n+1} &= A_n + \left(\frac{1-\varsigma}{\mathcal{Z}(\varsigma)} + \frac{3\varsigma h}{2\mathcal{Z}(\varsigma)}\right)\Upsilon_5(t_n, A_n) \\
&\quad + \left(\frac{\varsigma h}{2\mathcal{Z}(\varsigma)} - \frac{1-\varsigma}{\mathcal{Z}(\varsigma)}\right)\Upsilon_5(t_{n-1}, A_{n-1}) + {}^5R_n^{\varsigma},
\end{aligned} \tag{44}
$$

where the remainder terms satisfy

$$
\|{}^i R_n^{\varsigma}\|_{\infty} < \frac{\varsigma}{\mathcal{Z}(\varsigma)}(n+1)!h^{n+1}\mathcal{Z}, \quad i = 1, 2, 3, 4.
$$

6. Numerical simulations

In this section, we perform numerical simulations of the proposed HIV model under the fractional-order CF derivative. The initial conditions are set as $S(0) = 1000000$, $I(0) = 5000$, $C(0) = 800$, $T(0) = 550$ and $A(0) = 100$, with parameter values provided in Table 1. To evaluate the influence of key interventions on HIV control, we focused on four critical parameters: τ_I, ρ, ε_I, and ε_T. These parameters were analyzed directly to correspond to intervention strategies such as early diagnosis, adherence support, and viral suppression under antiretroviral therapy. Fig. 3 shows that increasing β increases R_0, whereas higher τ_I reduces R_0, demonstrating the importance of early treatment in limiting secondary infections. Fig. 4 displays that higher ε_I elevates R_0, while increasing τ_C reduces R_0, highlighting the impact of both infectiousness and timely treatment of chronic cases. Fig. 5 illustrates that R_0 increases with β and also rises with higher ρ, indicating that poor ART adherence can substantially undermine epidemic control.

Fig. 6 depicts the variation of the system across fractional orders $\varsigma = 0.70, 0.78, 0.88$, and 1.0. The results highlight the sensitivity of epidemic trajectories to the memory effect inherent in fractional dynamics, with lower ς values yielding slower decay in infection prevalence. Consequently, the recruitment rate initially exceeds the infection pressure, causing a temporary increase in the susceptible population before infection becomes dominant and $S(t)$ declines. Higher ς values behave similarly to the classical ($\varsigma = 1$) model, where infection spreads more rapidly and susceptible decline. Similarly, infection progression is slower due to memory effects, and the peaks of $I(t), C(t), T(t)$ and $A(t)$ occur in smaller magnitude.

Furthermore, in the fractional model (11), we varied the treatment initiation rate for acute infection (τ_I), the ART dropout rate (ρ), and the relative infectiousness of both acute and treated individuals (ε_I and ε_T). These parameters exert the strongest influence on memory-dependent

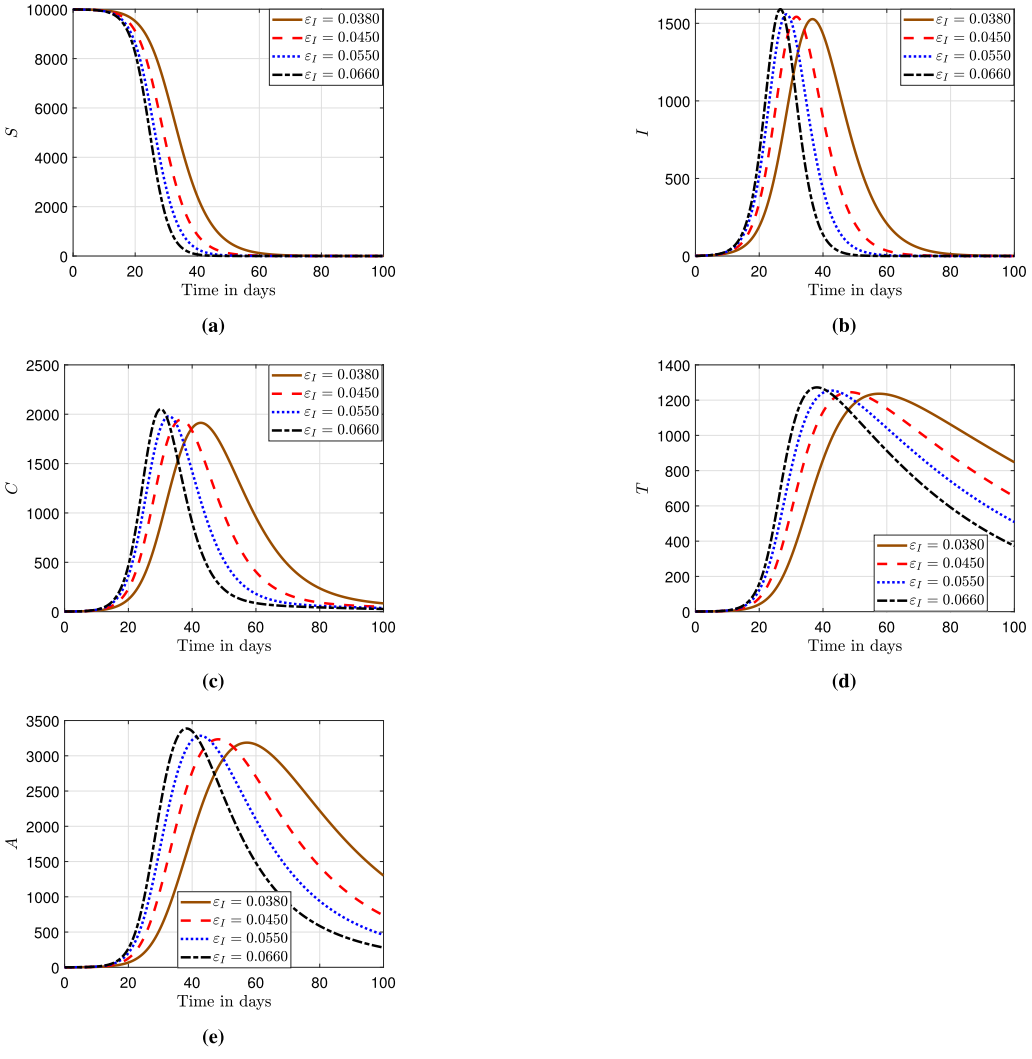

Fig. 10. Model behavior under fractional-order dynamics for ε_I, with the fractional order fixed at $\varsigma = 0.88$.

transmission dynamics. The impact of parameter variation on infection prevalence is illustrated in Figs. 7–10. Fig. 7 examines the effect of increasing the treatment initiation rate τ_I while keeping the fractional order fixed at $\varsigma = 0.88$. Increasing τ_I mitigates the epidemic peak, highlighting the importance of early treatment initiation in reducing HIV transmission.

Fig. 8 demonstrates that higher values of the treatment dropout rate ρ substantially diminish the benefits of therapy, as individuals who discontinue ART revert to a highly infectious state, leading to a resurgence in prevalence. Fig. 9 shows that reducing the relative infectiousness during the acute phase, ε_I, markedly suppresses epidemic intensity, highlighting the disproportionate contribution of acutely infected individuals to sustained transmission. Fig. 10 presents the effects of decreasing ε_T, reflecting improved viral suppression among treated individuals, which further diminishes long-term prevalence levels. These results indicate that early ART initiation, sustained retention in care, and enhanced viral suppression act synergistically to reduce onward transmission. This result highlights the pronounced sensitivity of outcomes to these parameters, underscores their pivotal role in shaping effective HIV control strategies, and provides a quantitative basis for prioritizing intervention policies.

7. Conclusion

In this study, we formulated and analyzed a five class HIV transmission model incorporating the CF fractional derivative. By combining the memory–dependent features of fractional calculus with classical compartmental modeling, the framework captures a richer and more realistic description of HIV dynamics. We established the existence and uniqueness of solutions, derived a bounded invariant region, and computed the basic reproduction number R_0 to characterize the epidemic threshold. Numerical results show that lower fractional orders slow the convergence to equilibrium, reflecting the influence of past infection history. The simulations further demonstrate that early ART initiation, strong adherence, and reduced dropout rates markedly suppress HIV transmission. Model parameters were estimated using the nonlinear least squares approach. The system is locally asymptotically stable when $R_0 < 1$ and globally stable when $R_0 > 1$, as shown using a suitable Lyapunov function. Solution stability was also examined using the UH criterion. Enhanced viral suppression among treated individuals amplifies these positive outcomes, leading to a sustained decline in HIV prevalence. Overall, the results highlight the joint influence of treatment strategies and memory effects on long term epidemiological dynamics, offering a quantitative basis for prioritizing targeted intervention strategies. Future work may extend this framework by incorporating optimal control formulations to assess cost effective prevention and treatment strategies under memory dependent transmission dynamics.

CRediT authorship contribution statement

Zakirullah: Writing – original draft. **Kamal Shah:** Investigation, Formal analysis. **M. Motawi Khashan:** Software, Methodology. **Bahaaeldin Abdalla:** Software, Investigation. **Thabet Abdeljawad:** Methodology, Investigation.

Funding

No funding was received for this work.

Declaration of competing interest

The authors declare that they have no known competing financial interests or personal relationships that could have appeared to influence the work reported in this paper.

Acknowledgement

Authors are thankful to Prince Sultan University for paying APC and providing support.

Data availability

No data was used in this paper.

References

[1] Baleanu D, Hasanabadi M, Vaziri AM, Jajarmi A. A new intervention strategy for an HIV/AIDS transmission by a general fractional modeling and an optimal control approach. Chaos Solitons Fractals 2023;167:113078.
[2] Barré-Sinoussi F, Chermann JC, Rey F, Nugeyre MT, Chamaret S, Gruest J, Dauguet C, Axler-Blin C, Vézinet-Brun F, Rouzioux C, Rozenbaum W. Isolation of a t-lymphotropic retrovirus from a patient at risk for acquired immune deficiency syndrome (AIDS). Science 1983;220(4599):868–71.
[3] World Health Organization. HIV and AIDS 15 Jul 2025. https://www.who.int/news-room/fact-sheets/detail/hiv-aids.
[4] Chinese center for disease control and prevention. Time Frame:1 November 2024 - 31 October 2025. https://www.chinacdc.cn/
[5] Xiao C, Jike C, Liu D, Jia P, Xu X, Xiao L, Yang S. The changing modes of human immunodeficiency virus transmission and spatial variations among women in a minority prefecture in southwest China: an exploratory study. Medicine 2020;99(6):e18776.
[6] Pang X, Wei H, Huang J, He Q, Tang K, Fang N, Liang S. Patterns and risk of HIV-1 transmission network among men who have sex with men in Guangxi, China. Sci Rep 2021;11(1):513.
[7] Zhu Q, Huang J, Wu X, Chen H, Shen Z, Xing H, Lan G. Virologic failure and all-cause mortality among older people living with HIV/AIDS in South China. AIDS Care 2023;35(12):1815–20.
[8] Feng S, Cheng WT, Li X, Luo XF. Contributions of the elderly to the transmission of HIV/AIDS in China. Infect Dis Model 2025;10(4):1488–506.
[9] Tahvi DF, Sokhan A. Global, regional, and national incidence, prevalence and mortality of HIV, 1980-2017, and projections to 2030, for 195 countries and territories: a systematic analysis for the global burden of diseases, injuries, and risk factors (GBD) 2017 study. 2019;6(12);e831–59.
[10] Hao Y, Luo Y, Huang J, Zhang L, Teng Z. Analysis of a stochastic HIV/AIDS model with commercial heterosexual activity and ornstein–uhlenbeck process. Math Comput Simul 2025;234:50–72.
[11] Meng R, Zheng T, Luo Y, Teng Z. Global attractor for an age-structured HIV model with nonlinear incidence rate. Appl Math Lett 2025;163:109428.
[12] Luo Y, Huang J, Teng Z, Liu Q. Role of ART and PrEP treatments in a stochastic HIV/AIDS epidemic model. Math Comput Simul 2024;221:337–57.
[13] Rihan FA. Numerical modeling of fractional-order biological systems. Abstr Appl Anal 2013;2013(1):816803. Hindawi Publishing Corporation.
[14] Eaton JW, Johnson LF, Salomon JA, Bärnighausen T, Bendavid E, Bershteyn A, Bloom DE, Cambiano V, Fraser C, Hontelez JA, Humair S. HIV treatment as prevention: systematic comparison of mathematical models of the potential impact of antiretroviral therapy on HIV incidence in South Africa. PLoS Medi 2012;9(7):e1001245.
[15] Hyman JM, Stanley EA. Using mathematical models to understand the AIDS epidemic. Math Biosci 1988;90(1–2):415–73.
[16] Odebiyi OA, Oladejo JK, Elijah EO, Olajide OA, Taiwo AA, Taiwo AJ. Mathematical modeling on assessing the impact of screening on HIV/AIDS transmission dynamics. J Appl Sci Environ Manag 2024;28(8):2347–57.
[17] Zanib SA, Ramzan S, Shah MA, Abbas N, Shatanawi W. Comprehensive analysis of mathematical model of HIV/AIDS incorporating fisher-folk community. Model Earth Syst Environ 2024;10(5):6323–40.
[18] Meetei MZ, DarAssi MH, Altaf Khan M, Koam AN, Alzahrani E, Ali H, Ahmadini A. Analysis and simulation study of the HIV/AIDS model using the real cases. Plos One 2024;19(6):e0304735.
[19] Yang Y, Li C, Fan X, Long W, Hu Y, Wang Y, Qu J. Effectiveness of omadacycline in a patient with chlamydia psittaci and KPC-producing gram-negative bacteria infection. Infect Drug Resist 2025:903–8.
[20] Xu Z, Li EH, Liu J, Zhang YJ, Xiao R, Chen XZ, Ding YB. Postpartum hemorrhage emerges as a key outcome of maternal SARS-cov-2 omicron variant infection surge across pregnancy trimesters. J Infect Public Health 2025;18(6):102733.
[21] Ullah MA, Raza N, Omame A, Alqarni MS. A new co-infection model for HBV and HIV with vaccination and asymptomatic transmission using actual data from Taiwan. Physica Scripta 2024;99(6):065254.
[22] Shi J, Liu C, Liu J. Hypergraph-based model for modelling multi-agent Q-learning dynamics in public goods games. IEEE Trans Netw Sci Eng 2024;11(6):6169–79.
[23] Liu B, Du H, Zhang J, Jiang J, Zhang X, He F, Niu B. Developing a new sepsis screening tool based on lymphocyte count, international normalized ratio and procalcitonin (LIP score). Sci Rep 2022;12(1):20002.
[24] Zhuang HH, Chen Y, Hu Q, Long WM, Wu XL, Wang Q, Xu TT, Qu Q, Liu YP, Xiao YW, Qu J. Efficacy and mortality of ceftazidime/avibactam-based regimens in carbapenem-resistant gram-negative bacteria infections: a retrospective multicenter observational study. J Infect Public Health 2023;16(6):938–47.
[25] Shukla A, Sukavanam N. Interior approximate controllability of second-order semilinear control systems. Int J Control 2024;97(3):615–24.
[26] Dineshkumar C, Udhayakumar R, Vijayakumar V, Nisar KS, Shukla A, Abdel-Aty AH, Mahmoud EE. A note on existence and approximate controllability outcomes of atangana–baleanu neutral fractional stochastic hemivariational inequality. Results Phys 2022;38:105647.
[27] Chauhan RP. Analyzing the memory-based transmission dynamics of coffee berry disease using caputo derivative. Adv Theory Simul 2025:e00373.

[28] Kumar S, Chauhan RP, Osman MS, Mohiuddine SA. A study on fractional HIV-AIDs transmission model with awareness effect. Math Methods Appl Sci 2023;46(7):8334–48.
[29] Almuallem NA, Chauhan RP. Effects of quarantine and vaccination on the transmission of lumpy skin disease: a fractional approach. PLoS One 2025;20(7):e0327673.
[30] Chauhan RP, Kumar S, Alkahtani BST, Alzaid SS. A study on fractional order financial model by using caputo–fabrizio derivative. Results Phys 2024;57:107335.
[31] Kumar S, Chauhan RP, Momani S, Hadid S. A study of fractional TB model due to mycobacterium tuberculosis bacteria. Chaos Solitons Fractals 2021;153:111452.
[32] Boulaaras S, Sriramulu S, Arunachalam S, Allahem A, Alharbi A, Radwan T. Chaos and stability analysis of the nonlinear fractional-order autonomous system. Alex Eng J 2025;118:278–91.
[33] Khan H, Alzabut J, Almutairi DK, Alqurashi WK. The use of artificial intelligence in data analysis with error recognitions in liver transplantation in HIV-AIDS patients using modified ABC fractional order operators. Fractal Fract 2024;9(1):16.
[34] Selvam A, Boulaaras S, Sabarinathan S, Radwan T. Nonlinear fractional order financial system: chaotic behavior and ullam hyers stability. Fractals 2025;33(4):2540082.
[35] Selvam A, Sabarinathan S, Khan H, Alzabut J, Gómez-Aguilar JF. Numerical simulation of ebola transmission disease dynamics using fractional derivatives involving real data for more effective prediction. Int J Model Simul Sci Comput 2025;2550062.
[36] Selvam A, Sabarinathan S, Senthil Kumar BV, Byeon H, Guedri K, Eldin SM, Govindan V. Ullam hyers stability of tuberculosis and COVID-19 co-infection model under Atangana-Baleanu fractal-fractional operator. Sci Rep 2023;13(1):9012.
[37] Ullah I, Bilal M, Shah D, Khan H, Alzabut J, Alkhawar HM. Study of nonlinear wave equation of optical field for solotonic type results. Partial Differ Equ Appl Math 2025;13:101048.
[38] Fatmawati, Boulaaras S, Arunachalam S, Sriramulu S. Results on Ulam-Hyers stability of nonlinear chen system with fractional-order derivative. Asian J Control 2025.
[39] Khan MA, Odinsyah HP. Fractional model of HIV transmission with awareness effect. Chaos Solitons Fractals 2020;138:109967.
[40] Jajarmi A, Baleanu D. A new fractional analysis on the interaction of HIV with CD4+ T-cells. Chaos Solitons Fractals 2018;113:221–9.
[41] Pinto CM, Carvalho AR. Fractional modeling of typical stages in HIV epidemics with drug-resistance. Prog Fract Differ Appl 2015;1(2):111–22.
[42] Mani G, Gnanaprakasam AJ, Ramalingam S, Omer AS, Khan I. Mathematical model of the lumpy skin disease using caputo fractional-order derivative via invariant point technique. Sci Rep 2025;15(1):9112.
[43] Moore EJ, Sirisubtawee S, Koonprasert S. A caputo–fabrizio fractional differential equation model for HIV/AIDS with treatment compartment. Adv Differ Equ 2019;2019(1):1–20.
[44] Lu C, Li L, Shah K, Abdalla B, Abdeljawad T. Mathematical insights into chaos in fractional-order fishery model. Model Earth Syst Environ 2025;11(3):1–17.
[45] Caputo MR, Ling C. Intrinsic comparative dynamics of locally differentiable feedback stackelberg equilibria. Dyn Games Appl 2015;5(1):1–25.
[46] Losada J, Nieto JJ. Properties of a new fractional derivative without singular kernel. Progr Fract Differ Appl 2015;1(2):87–92.
[47] Cai C, Tang H, Li D, Qin Q, Chen F, Jin Y, Lyu F. Evolution of HIV epidemic and emerging challenges—China, 1989–2023. China CDC Wkly 2024;6(48):1251.
[48] National bureau of statistics, 2004. https://www.nigerianstat.gov.ng.
[49] Health official. China daily; 2024. https://en.nhc.gov.cn/2025-03/10/c_86403.htm.
[50] Center for Health Data Science. https://e.huawei.com>industries>commercial-market.
[51] Van den Driessche P, Watmough J. Reproduction numbers and sub-threshold endemic equilibria for compartmental models of disease transmission. Math Biosci 2002;180(1–2):29–48.
[52] Ulam SM. Problems in modern Mathematics. Courier Corporation; 2004.
[53] Hyers DH. On the stability of the linear functional equation. Proc Natl Acad Sci 1941;27(4):222–4.
[54] Atangana A, Owolabi KM. New numerical approach for fractional differential equations. Math Model Nat Phenomena 2018;13(1):3.

Author biography

Zakirullah: PhD Scholar in School of Mathematical Sciences, University of Electronic Science and Technology of China, Chengdu, 611731, China. His research area is related to mathematical modeling and numerical simulations.

Kamal Shah: He is senior researcher at Prince Sultan University Saudi Arabia. Before, he was associate professor in University of Malakand Pakistan. He has been listed in top 2% research scientist in Stanford list for career long during 2025. His research area devoted to fractional calculus, fuzzy analysis, mathematical modeling and numerical analysis.

M. Motawi Khashan: He is an Associate Professor of Mathematics at King Saud University, specializing in Differential Geometry and Mathematical Modeling. He earned his Ph.D. from the Western University of Timisoara, Romania (2002). With over 20 years of academic experience, Dr. Khashan has published more than 27 peer-reviewed papers in ISI and Scopus-indexed journals, covering areas such as fractional calculus, numerical analysis, and differential equations. Beyond research, he serves as the coordinator for “Principles of Statistics and Probability” at the Common First Year Deanship and is an accredited Peer Consultant in Teaching. A recipient of the King Saud University Award for Excellence in Teaching (2012), he has also authored and translated several mathematical textbooks. His current interests focus on enhancing technology-enhanced learning and mathematical modeling.

Bahaaeldin Abdalla: Associate professor at Prince Sultan University Saudi Arabia. His research work is related to differential geometry and analysis.

Thabet Abdeljawad: He is professor at Prince Sultan University Saudi Arabia. His main research work devoted to fractional calculus, Modeling and fixed point theory. He has been listed in top 2% research scientist in Stanford in the last 5 years list for career long. He was alos listed in 1% higly cited announced by Clarivate in the years 2019, 2020, and 2021.